# EVOLUTION OF POLYTHENE SHEET PERFORMANCE ON THE BEARING CAPACITY OF SOFT SOIL



**By**

**Muhammad Fazeel**

**NUST- 2017-MS-Geotech-00000205574**

A thesis submitted in partial fulfillment of the requirements for the degree of

Master of Science in Geotechnical Engineering

**NUST Institute of Civil Engineering (NICE)**

**School of Civil and Environmental Engineering (SCEE)**

**National University of Sciences and Technology (NUST)**

**H-12 Sector, Islamabad, Pakistan**

**2020**

By

**Muhammad Fazeel**

**NUST- 2017-MS-Geotech-00000205574**

A Thesis submitted in partial fulfillment of

the requirements for the degree of

**Master of Science**

**In**

**Geotechnical Engineering**

**NUST Institute of Civil Engineering (NICE)**

**School of Civil and Environmental Engineering (SCEE)**

**National University of Sciences and Technology (NUST)**

**H-12 Sector, Islamabad, Pakistan**

**2020**

# PLAGIARISM DECLARATION

i.     I know the meaning of plagiarism and declare that all the work in the document, save for that which is properly acknowledged, is my own. This thesis/dissertation has been submitted to the Turnitin module (or equivalent similarity and originality checking software) and i confirm that my supervisor has seen my report and any concerns revealed by such have been resolved with my supervisor.

ii.    I have used the NUST Synopsis and Thesis Manual as Author-date-referencing-guide based on the APA convention for citation and referencing. Each significant contribution and quotation in this dissertation from other work /research has been attributed and has been cited and referenced, accordingly.

iii.   This dissertation is my own work.

iv.    I have not allowed and will not allow anyone to copy my work with the intention of passing it as his or her own.


Signature: _____          Date:

Student Name: **<u>Muhammad Fazeel</u>**

# THESIS ACCEPTANCE CERTIFICATE

Certified that final copy of MS thesis written by **MUHAMMAD FAZEEL (Registration No. NUST- 2017-MS-Geotech-00000205574)** of **NUST INSTITUTE OF CIVIL ENGINEERING (NICE)** has been vetted by undersigned, found complete in all respects as per NUST Statutes/Regulations, is free of plagiarism, errors, and mistakes and is accepted as partial fulfillment for award of MS degree. It is further certified that necessary amendments as pointed out by GEC members of the scholar have also been incorporated in the said thesis.

Signature: _____
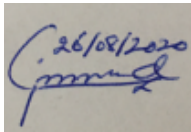
Name of Supervisor: **Dr. Tariq M. Bajwa**

Date: _____

Signature (HoD): _____

Date: _____

Signature (Dean/Principal):_____

Date: _____

This is to certify that the

Thesis titled

# EVOLUTION OF POLYTHENE SHEET PERFORMANCE ON THE BEARING CAPACITY OF SOFT SOIL

Submitted by

**Muhammad Fazeel**

has been accepted towards the partial fulfillment

of

the requirements

for

Master of Science in Geotechnical Engineering
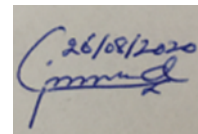
_____

**Dr. Tariq M. Bajwa**

**(Thesis Supervisor)**

**Assistant Professor**

**NUST Institute of Civil Engineering (NICE)**

**THIS THESIS IS**

**DEDICATED**

**TO**

**MY BELOVED PARENTS**

**&**

**MY WIFE**

(For their endless love, support and encouragement)

# ACKNOWLEDGEMENT

**Table of Contents**

# List of Figures

# List of tables

# ABSTRACT

There are certain situations in the field compelling the engineers and scientists to enhance the bearing capacity of weak soils due to their lower strength to bear the superstructure loads. It is always preferred to use higher bearing capacity soils i.e., coarse-grained soils in foundations, but sometimes, it is unavoidable to use lower bearing capacity soils, i.e., soft soils due to unavailability of higher strength soils in the vicinity of the project area, and it is really expansive to borrow soils from remote areas. The soft soil undergoes excessive deformation on wetting and under the application of loads. In this situation, it is more feasible to improve the bearing capacity of soft soil, used in foundations. So, the objective of this study is to strengthen the soft soil foundations with partial layers of sand and polythene reinforcement. The potential benefits of polythene reinforcement were examined, conducting seven small-scale physical model tests and forty-seven numerical simulations with a square footing, sustained on medium dense sand and overlying soft clay. First, the data sets of numerical simulation were validated by comparison with the physical model test results, in which a good agreement was found. Finally, a detailed parametric study was executed using a finite element analysis to figure out the best alternative for number of reinforced layers ($N$), effective depth of reinforcement ($d$), thickness of top sand layer ($Ds$), in-between spacing of alternate reinforcements ($h$), top spacing of reinforcement ($u$) and reinforcement length ($b$). The test results showed that the soil system reinforced with 03 polythene layers provided the peak ultimate bearing capacity to that of other alternatives. Design recommendations are suggested on the basis of finite element model and the laboratory model studies for a square rigid footing supported on a reinforced granular fill – soft soil system.

# 1. INTRODUCTION

## 1.1. Background

The innovations in the civil engineering industry are taking place quite rapidly due to global modernization and with a rapid increase in population throughout the world. The engineers, scientists, and policy makers are making their best efforts to introduce new technologies to accommodate this growing population and modernized industrialization on economic and efficient grounds. Regarding this, there is a huge focus to construct high-rise buildings in order to lessen the use of open spaces. Foundation is the most critical component of any infrastructure as it transforms the load of the superstructure to the basal soil, so its safe and economical design in any civil engineering project is highly important. It is highly feasible to use higher bearing capacity soils (coarse-grained soils) in foundations, but sometimes, it is unavoidable to use lower bearing capacity soils (soft soils) due to the unavailability of higher strength soils in the vicinity of the project area.

The soft soil has lower strength and undergoes excessive deformations on wetting and under the application of loads. Generally, the soft clay shows higher water content, closer to the liquid limit with undrained shear strength between 10 and 50 kPa (Terzaghi and Peck, 1967). Most commonly, these types of soils fall in the category of problematic soils, showing loose formation with higher swelling or shrinkage potential due to the presence of higher percentage of montmorillonite (Viswanadham et al., 2009). The foundation soil needs to be durable enough to bear the super structure load without settlement and shear failure. In this scenario, it is really important to enhance the bearing capacity of soft soils to be used in foundations.

Regarding this, various studies report different approaches such as biological, chemical, and mechanical stabilizations etc., to enhance the bearing capacity of soft soils. Furthermore, these researchers employed different experimental and numerical approaches to examine the behaviour of these soils. (Ghalehjough et al., 2017)

executed the ultimate bearing capacity of a strip footing replacing soft soil with three different types of granular materials including, angular, rounded, and well rounded, and concluded that the angular soil particles provided higher strength than that of other types. (Tafreshi and Dawson, 2010) executed the bearing capacity of geosynthetic in combination with granular materials and clayey soils in foundations and reported that the bearing capacity was about 50% more for two layers of granular materials as compared to one layer. (Zukri et al., 2017) performed experimental investigations using fibers in order to improve the engineering properties of clayey soil. (Chen, 2007) derived a numerical expression for the general failure zone and reported that the geosynthetic enabled to increase the lateral stress between the active and passive wedges, which enabled to minimize the general failure within the reinforced zone.

However, in the current study, the soft soil is strengthened with partial layers of polythene reinforcement in combination with granular fills, which is in contrast to the previous research studies to use materials such as geotextile, geomembrane, and geocells etc., to reinforce the footing resting on a soil system. The study employs physical and numerical simulation models to examine the performance of composite soil system for several combinations such as number of polythene reinforcement layers, thickness of partial layers of sand and clay, thickness of sand layer, in-between spacing of polythene, and top layer spacing of polythene etc. Finally, several concluisons of practical interest are derived form the study.

## 1.2. Problem statement

Regarding this, various studies reported different approaches such as biological, chemical and mechanical stabilizations etc., to enhance the bearing capacity of soft soils in foundations. However, in the current study, the authors introduce a model to improve the bearing capacity of soft soils in foundations in combination with polythene sheeting and granular materials. The research in this field, specifically, the use of polythene sheeting is quite minimal. The polythene bags release hazardous contaminants such as nitrogen oxides and sulfur dioxide to the atmosphere, posing adverse impacts to the humans and wildlife as well. As per

research studies, polythene sheeting needs high-energy ultra-violet light for its decomposition or breakdown, and their average life is almost 100 years.

## 1.3. Objectives of the study

The objectives of the study are as:

1. To investigate the bearing capacity of soft soil foundations, partially strengthened with polythene reinforcement and granular materials, developing small-scale physical and numerical simulation models.

2. To testify the polythene sheet as a reinforcement material in foundation soils.

## 1.4. Justification of the study

The concept of high-rise commercial and domestic buildings is prevailing throughout the world and in Pakistan too, due to the rapid increase in population and the industrial revolution. In this situation, higher bearing capacity soils are needed to support the superstructure loads, efficiently and economically. Sometimes, higher bearing capacity soil is not available at the project site such as lower Punjab Pakistan, so, in this situation, it is more feasible to improve the performance properties of existing soils through chemical or mechanical means. Polythene sheeting is the most widely used synthetic plastic in the world (Zukri et al., 2017) and in Pakistan as well (Nasir et al., 2014), showing its detrimental impacts on the environment too. Pakistan annually produces 300 million tons of polythene bags. So, this study testifies the use of polythene sheeting in combination with clay and granular soils to improve the performance properties of the foundation soils.

## 1.5. Thesis outlines

The chapters in this thesis are outlined as;

1. Chapter 1 highlights the research background, problem statement, objectives, and the justification of the research work.

2. Chapter 2 represents a detailed literature review, relating to the research work.

3. Chapter 3 elaborates the materials used and the methods adopted to conduct the research study.

4. Chapter 4 reports the results and discussions, drawn from the research work, highlighting the validation of the physical data sets with the numerical data sets.

5. Chapter 5 represents the conclusions with few key recommendations, drawn from the study.

# 2. LITERATURE REVIEW

## 2.1. General

The term "soft clay" is defined as silty clay or clayey soil that comes to equilibrium by its own weight but not undergoes significant secondary consolidation since its development. Soft clays usually show higher amount of water contents, nearly close to the liquid limit, due to which, these types of soils are regarded as relatively loose formation (Bjerrum, 1967).

Soft soil is extensively located in coastal regions, showing significant compressibility and lower strength. The soft soil deposits, most commonly, exhibited lower shear strength and excessive settlement, while used in construction (Barksdale and Bachus, 1983). (Terzaghi, 1936) reported that a soft clay showed a liquid index (L.I.) > 0.5 and undrained shear strength ($C_u$) < 10 kPa whereas (Terzaghi and Peck, 1967) defined the unconfined compressive strength ($C_u$) of soft soil between 12 and 50 kPa. However, (Brand and Brenner, 1981) classified a soft clay with $C_u$ < 40 kPa. According to (B.S: C.P 8004: 1986) standard, a soil is classified as a soft soil if its undrained shear strength is < 40 kPa and > 20 kPa, and a soil with $C_u$ < 20 kPa is referred to a very soft clay. According to the German Geotechnical Society, a soil behaves as a soft soil for constructional purposes as per criteria if., i-) consistency index < 0.75, ii-) the soil is fully saturated or near to full saturation, and iii-) undrained shear strength < 40 kPa.

## 2.2. Soil characterization

### 2.2.1. Grain size distribution

The grain size distribution of soil particles provided significant effects on the engineering behavior of all soils (Tyler and Wheatcraft, 1992)., e.g., the uniformly

graded soils are used to control drainage applications as not susceptible to loss of fines by internal erosion. Hydraulic conductivity in certain applications can also be maintained within definable and narrow limits on the basis of grain size distribution. Thus, it is essential to define the particular size of particles in the soil sample, accurately. Sieve analysis and hydrometer tests are generally conducted to categorize the grain size distribution of soils. Equations 2.1 and 2.2 are used to define the coefficient of uniformity ($C_u$) and coefficient of curvature ($C_c$) of sand, respectively for practical applications (Das, 2013).

$$C_u = \frac{D_{60}}{D_{10}} \qquad\qquad (Eq-2.1)$$

$$C_c = \frac{(D_{30})^2}{D_{60} \; x \; D_{10}} \qquad\qquad (Eq-2.2)$$

Here $D_{10}$, $D_{30}$, and $D_{60}$ represent the diameters of sieve through which the 10 percent, 30 percent, and 60 percent of the total sand mass passes respectively.

### 2.2.2. Atterberg limits

The presence of water in the voids of the clay influences the engineering behavior of fine-grained soil. The water content associated with Atterberg limits of the fine soil, predicts the engineering response of the particular soil**.** (Smith et al., 1985) reported that these limits enabled to classify the engineering properties of soil. A soil exhibited non-cohesive nature at the lower plastic limit and cohesive nature at the higher plastic limit, and provided large volume variations due to absorb and release of water (Seed et al., 1966). The consistency index (C.I.) shows the firmness of the soil sample and is calculated, using Equation 2.3.

$$C.I = \frac{LL-w}{LL-PL} \qquad\qquad (Eq-2.3)$$

### 2.2.3. Compaction

The standard and modified proctor tests are generally performed to determine the optimum moisture content and maximum dry density (Juran and Guermazi, 1988).

Generally, shallow foundations are built upon the controlled fill, known as structure fill or engineering fill. Different researchers used different methods to attain the desired density of the clayey soil; and researchers (Sakti and Das, 1987; Hamed, 2001; Kolay et al., 2013) employed hand hammers for this purpose, whereas other researchers (Siddiquee, 1991; Shiau et al., 2003; Latha and Somwanshi, 2009; Abu-Farsakh et al., 2013) used falling head method, vibratory hammer method, raining method, relative density method, and sand replacement method for non-cohesive soil.

### 2.2.4. Shear strength

The shear strength parameters (cohesion and angle of internal friction) are considered highly important to figure out the bearing capacity and settlement of foundation soils (Das, 1983). These parameters play a key role in the safety design of any geotechnical construction work. (Nagendra et al., 2013) reported that soils failed, when selected improper values of these parameters, irrespective of the soil conditions.i.e, soft, stiff or firm. A direct shear test is an easy and economically effective method, to find out the cohesion and friction angle of soil.

### 2.2.5. Specific gravity

Specific gravity is defined as the density of the soil solid to the density of the water. Generally, the specific gravity varies from 2.6 to 2.75 for the non-organic soil.

### 2.2.6. Unconfined compressive strength

The unconfined compression test is generally employed to estimate the unconfined compressive strength of the saturated cohesive soil. This test guessed the failure pattern only, as the effective strength parameter remained unknown due to no pore water pressure measurement (Sherif and Burrous, 1969). Table 2.1 shows unconfined compressive strength of soils with various consistencies (Bowles, 1996).

Table 2.1: Cohesive soil consistency

| Consistency | Unconfined Compressive Strength (kPa) |
|---|---|
| Very Soft | Less than 24 |
| Soft | 24 to 48 |
| Medium stiff | 48 to 96 |
| Stiff | 96 to 192 |
| Very stiff | 192 to 383 |
| Hard | Greater than 383 |

### 2.2.7. Undrained shear strength - Portable vane shear

The portable vane shear test is a rapid and easy method to determine the undrained shear strength of the soft soil (Young et al., 1988). The device is generally employed to determine the approximate undrained shear strength of the saturated cohesive soil; however, the presence of coarse material in soil adversely affected the test result (ASTM D-8121). (Ismail Ibrahim, 2016) conducted portable vane shear (PVS) tests to determine the in situ undrained shear strength of cohesive soil at different moisture contents. In the current study, the vane shear tests were conducted to determine the undrained shear strength of soft state cohesive soils.

### 2.2.8. Swelling behavior

(Viswanadham et al., 2009) classified the expensive soils as problematic soils due to their higher swelling potential, and the structures constructed on these types of soils experienced great damages and distresses. Table 2.2 classifies the degree of swelling from the swelling index of the soil as reported by (Mohan and Goel, 1959). (Seed and Lundgren, 1962) classified the degree of expansion from the swelling potential (Table 2.3). (Gromko, 1974) stated that a soil exhibited swelling potential if i-) its moisture content is close to the plastic limit, and ii-) the montmorillonite is present in the soil sample. (Ashayeri and Yasrebi, 2009) classified a relationship between index properties and the swelling behaviour, based on the data sets of five different clays having low to high plasticity.

Table 2.2: Classification of the expansion from the free swell index

| Liquid limit (%) | Plasticity index (%) | Free swell index (%), FSI | Degree of expansion | Degree of severity |
|---|---|---|---|---|
| 70–90 | >32 | >200 | Very high | Severe |
| 50–70 | 23–32 | 100–200 | High | Critical |
| 35–50 | 12–23 | 50–100 | Medium | Marginal |
| 20–35 | <12 | <50 | Low | Non critical |

Table 2.3: Degree of expansion based on the swelling potential

| Degree of expansion | Swelling potential (%) |
|---|---|
| Very high | >25 |
| High | 5–25 |
| Medium | 1.5–5 |
| Low | 0–1.5 |

## 2.2.9. Activity

The change in volume during the swelling is dependent upon the plasticity index (P.I.) and the percentage of clay fraction in the soil sample (Skempton, 1953). Activity is an index property, used to define the swelling behavior of expensive soil. Table 2.4 classifies the nature of the soil on the basis of the activity (Asuri and Keshavamurthy, 2016).

Table 2.4: Activity based expensive soil classification

| Activity ($A_c$) | Nature of the soil | Probable degree of swell potential |
|---|---|---|
| <0.75 | Inactive | Low |
| 0.75–1.25 | Normal | Medium |
| >1.25 | Active | High |

The low activity soil such as kaolinite provided lower swelling and shrinkage whereas soil containing montmorillonite produced higher volume changes (Asuri and Keshavamurthy, 2016). Figure 2.1 classifies kaolinite, illite, and montmorillonite minerals with respect to activity and percentage of the clay fraction.
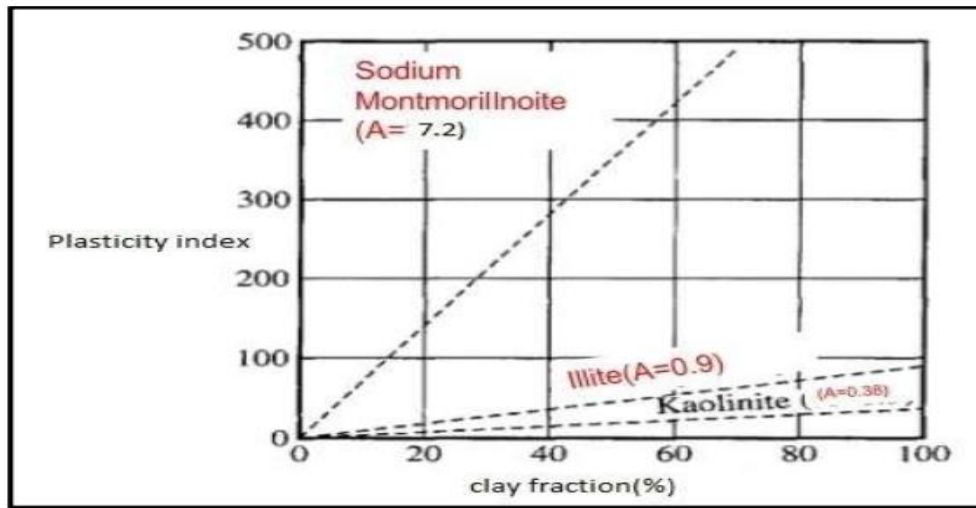
Figure 2.1: Activity of different clay minerals for clay fraction and plasticity index

## 2.2.10. Minimum and maximum void ratio

The evaluation of the maximum and minimum void ratio is necessary to predict the packing characteristics of the fine-grained sand. For the strength of soil, relative density has a correlation with the void ratios of the sand (Cornforth, 1973). (Ghalehjough et al., 2017) conducted an experimental study to check the influences of roundness and angularity of the granular materials; and suggested that $e_{min}$ and $e_{max}$ decreased with an increase in roundness and increased with an increase in angularity. The state of compaction with the relative density is presented in Table 2.5.

Table 2.5: State of compaction with relative density

| Relative Density $D_r$ (%) | State of compaction |
|---|---|
| 0 - 15 | Very loose |
| 15 - 35 | Loose |
| 35 – 65 | Medium dense |
| 65 – 85 | Dense |
| 85 - 100 | Very dense |

## 2.3. Ultimate bearing capacity of footing resting on stratified deposits of soil

The design of foundation needs to be fulfilled the standards of serviceability and strength, and it needs to durable enough to carry out the structure loads within the permissible limits of settlement and shear failure. Deformation takes place in the soil mass with a gradual increase in the specific load. Various parameters such as embedment, shape, size of the footing, and layer thicknesses etc., define the failure mechanism in foundation soil for an applied load. Therefore, it is essential to consider the above-mentioned parameters in the design of the soil's bearing capacity. It is assumed that the subsoil is homogenous and isotropic, during the theoretical analysis of all real problems. Generally, in nature, the soil is a mixture of clay, silt, and sand in varying proportions, highlighting it as a heterogeneous and anisotropic material. (Abu-Farsakh et al., 2013) tested a soil with partial layers of distinct strengths and composition characteristics and verified that the homogeneity assumption is not valid based on the failure surfaces covering the boundaries of the layers.

Button (1953) gave the concept of analyzing the bearing capacity of a layered soil system, and (Brown and Meyerhof, 1969) proved that, the analysis of layered soil systems by Button gave conservative results. Furthermore, (Vesic, 1975) interpolated the test data of (Brown and Meyerhof, 1969), and presented a theory relative to the layered soil system. (Meyerhof, 1974) presented equations and theories, conducting the model tests on two-layered soil system, i.e., stiff clay underlying loose sand and soft clay underlying dense sand, and the research was further proceeded by (Meyerhof and Hanna, 1978) conducting more model tests on the layered soil systems.

Various studies reported different approaches to enhance the performance properties of the weak foundation soil, but one of the most common methods are employed to replace the soft soil with some higher strength materials such as granular materials in partial layers to reinforce a weak foundation soil. Several studies were carried out in this respect to enhance the bearing capacity of foundation soils underneath

a footing. First of all, (Madhav and Vitkar, 1978) presented an idea of replacing the soft foundation materials with higher strength materials which were proceeded by (Eun Chul Shin and Das, 1998). After then, (Madhav and Vitkar, 1978) introduced the first formulation in this filed which was physically verified by (Hamed, 2001).

(Al-Suhaily) developed a model to examine the bearing capacity of soft soil (CL), replacing it with granular materials, and concluded that the rectangular (trench) pattern provided higher strength than that of a square pattern. However, (Ibrahim, 2016) showed that the ultimate bearing capacity was directly proportional to the thickness and angle of internal friction of granular soil, and the foundation depth as well, and was inversely proportional to the diameter of the footing.

(Ghalehjough et al., 2017) executed the ultimate bearing capacity of a strip footing replacing soft soil with three different types of granular materials including, angular, rounded and well-rounded, and concluded that the angular soil particles provided higher strength as compared to other types. In addition to this, the study also discussed the ultimate bearing capacity of footing for various ranges of roundness, particle size and relative density, and reported that the ultimate bearing capacity increased with an increase in particle size and relative density, however, the effect of roundness on the bearing capacity of footing was observed insignificant.

(Ornek et al., 2012) conducted field investigations to examine the influence of shape and size of the footing on the bearing capacity of the soil, selecting three different layers of granular materials. It was noticed that the bearing capacity of footing increased with an increase in footing size and thickness of the granular fill as well. (Taylor, 1995) worked on scale effect to predict the foundation width to grain size ratio of foundation and reported that the acceptable size ratio ($B/D_{50}$) was greater than 100. While the scale effect showed a significant effect on the bearing capacity of the soil if $B/D_{50}$ ratio was less than 50-100, where $B/D_{50}$ represents foundation width to grain size ratio.

Abdul-Baki et al. (1993) examined the bearing capacity of soft soil foundation, strengthened with granular materials for eccentric, concentric, and inclined loadings.

The test data showed that the bearing capacity of the reinforced soils was estimated about three times more than the unreinforced ones for all loadings. The study further added that the bearing capacity increased gradually for a length up to 1.25$B$ for granular materials but after this, the increase in BC was observed minimal. (Kenny and Andrawes, 1997) presented theoretical models, executing small scale laboratory model tests for different conditions, i-) sand only, ii-) clay only and iii-) sand overlying the clay deposit, and reported that the foundation soils exhibited local shear failure for sand overlying the clayey layer.

(Merifield et al., 1999) employed semi-empirical and empirical approaches to investigate the bearing capacity of layered soils using undrained conditions and reported that various layered soil system exhibited different failure mechanisms, which were dependent on the partial thicknesses of the layers. Numerical modeling was done by Plaxis using parameters including c and $\phi$ for the soil plasticity, E and $v$ for the soil elasticity and $\psi$ for the dilatancy angle of the soil to test the bearing capacity of foundation soil. The test data showed that the bearing capacity of the foundation soil increased with an increase in the layer thickness of the granular materials, and furthermore, a good agreement was found between the finite element model and the physical model test results, both with and without replacement. The authors further examined the influences of scale effect on footing size, conducting field testing. In the study, different footing diameters (1.2, 1.5, 3.0, 6.0, 12.0, and 25.0 m) for different granular thicknesses (1.33$D$, 1.67$D$, and 2.00$D$) were employed. The study concluded that the effects on footing size were less significants, for footings placed on the clayey bed as compared to the footings placed on the granular materials, showing its relevancy to $B/D_{50}$ ratio.

## 2.4. Geosynthetic reinforced foundation

In certain situations, it is imperative to enhance the bearing capacity of weaker soils in the foundation, incorporating different layers of geosynthetic materials within the soil matrix, in addition to the partial layers of granular materials. According to

(Mandal and Sah, 1992) reported that the bearing capacity of the foundation soil increased for two to four layers of the geosynthetic reinforcements, which were within the effective zone of foundation soil. The study further added that the tensile resistance of the geosynthetic enabled the shear stress to distribute over a larger area which resulted in an increase in the bearing capacity. Different types of reinforcements including geotextile, geomebrane, and polythene are generally used in the foundation soil. In addition to this, (Chen, 2007) reported to use filler materials such as fly ash, sand, and aggregate etc., to strength the foundation soils.

### 2.4.1. Failure modes of geosynthetic reinforced foundations

(Binquet and Lee, 1975) and (Huang and Menq, 1997) stated that a geosynthetic reinforced foundation exhibited six potential failure modes (Figure 2.2). Shallow failure happens above the uppermost reinforcement when the fill is too weak and the spacing from the first geosynthetic reinforcement layer to the footing base is too wide as shown in Figure 2.2 (a). The interlayer failure between reinforcement occurs when the in-between spacing of consecutive layers of the geosynthetic is too large (Figure 2.2 (b)). The general failure develops within the reinforced zone, when multiple reinforcement layers are used in thicker layers within the replaced material in foundation soil as shown in Figure 2.2 (c). When the zone of the reinforcement is thin and wide and the underlying soil is weak in foundation soil, then the applied stresses initiate to distribute from the footing base, extending towards the weaker soil, and consequently, failure of distributed foundation soil takes place as shown in Figure 2.2 (d). Punching failure through reinforced zone occurs when the reinforcement in the foundation is limited and thinner, and the weaker soil is present at the bottom (Figure 2.2 (e)). Punching failure of the reinforced zone through the week soil happens when the reinforcement in the foundation soil is thin and narrow within the weaker soil at the bottom (Figure 2.2 (f)).

(a) Shallow failure above uppermost reinforcement  (b) Interlayer failure between reinforcements  (c) General failure within reinforced zone

(d) Failure of distributed foundation  (e) Punching failure through reinforced zone  (f) Punching failure of reinforced zone
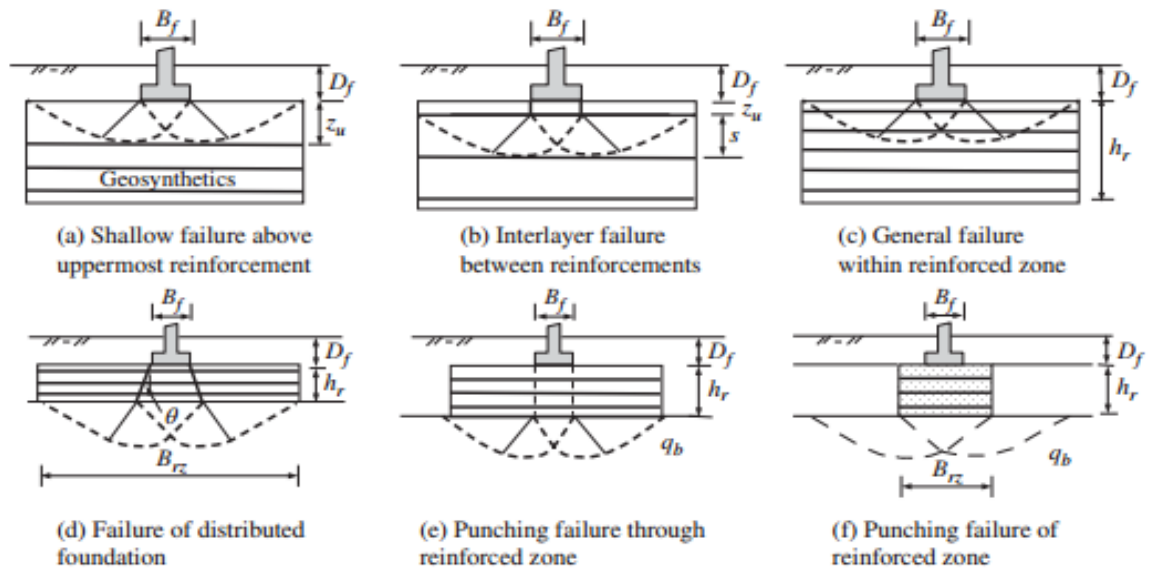
Figure 2.2: Potential failure modes of geosynthetic reinforced foundation

## 2.4.2. Remedial measures for different failure modes

### 2.4.2.1. Bearing capacity for shallow failure

(Binquet and Lee, 1975) reported that a shallow failure occurred in the geosynthetic reinforced foundation soil in case of $u/B_f > \frac{2}{3}$. The slip surface can be restricted within the reinforced zone, placing the 1$^{st}$ layer of the reinforcement close to the bottom of the footing to avoid such types of failures. (Wayne et al., 1998) developed a relationship between $u/B_f$ and bearing capacity ratio for different friction angles to eliminate or minimize the chances of shallow failure in foundation soil (Figure 2.3).
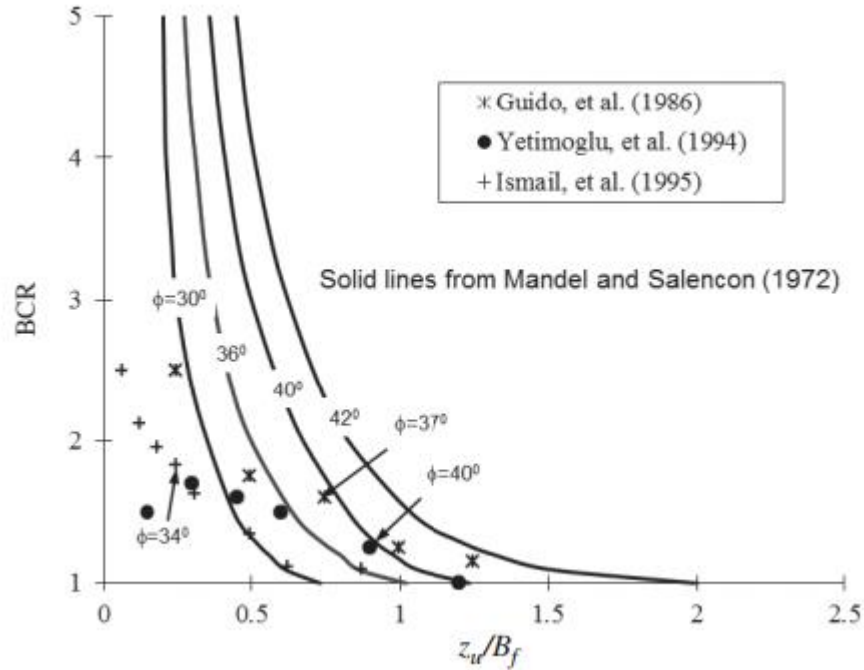
Figure 2.3: Relationships between *BCR* and $u/B_f$ of soils for different friction angles

## 2.4.2.2. Bearing capacity for interlayer failure

For interlayer failure, the UBC can be improved through the side resistance of the punching wedge, tensile effect of the uppermost reinforcement, and the base resistance. When uppermost distance ($u$) is equal to or greater than the spacing between two consecutive reinforcement layers ($h$), the UBC of footing against the interlayer failure is presumed to be sufficient against the interlayer failure (Han, 2015).

## 2.4.2.3. Bearing capacity for general failure within the reinforced zone

Generally, a general failure within the reinforced zone occurs in a foundation soil of multiple thicker reinforcement layers (Figure 2.2 (c)). (Chen, 2007) derived a numerical expression for the general failure zone and reported that the geosynthetic enabled to increase the lateral stress between the active and passive wedges, which enabled to minimize the general failure within the reinforced zone. Equation 2.4 represents a general expression for UBC as reported by (Chen, 2007)

$$q_{ult,r} = q_{ult,u} + \Delta q_T \qquad\qquad (Eq - 2.4)$$

Where $\Delta q_T$ represents an increase in the bearing capacity, due to the geosynthetic reinforcement tensile resistance.

### 2.4.2.4. Bearing capacity for distributed foundation failure

Huang and Menq (1997) presented an analytical method for load spread angle to examine the bearing capacity of distributed foundation failure, and (Wayne et al., 1998) reported spread angles of 26.7º and 45º for unreinforced and reinforced foundation soils respectively, to minimize the chances of distributed failure.

### 2.4.2.5. Bearing capacity for punching failure through the reinforced zone

To prevent this failure, the geosynthetic reinforcement needs to be provided on the larger area, which consequently increases $q_u$ against punching failure due to its base resistance, side resistance, and tensile effects.

### 2.4.2.6. Bearing capacity for punching failure of the reinforced zone

Lawton (2001) reported an analytical solution to enhance the bearing capacity of foundation soil against punching failure for the reinforced portion (Equation - 2.5)

$$B_{rz} > B_f + 2h_r \tan\theta_s \qquad\qquad (Eq - 2.5)$$

Where $\theta_s$ is the distributed angle, determined from the modulus of elasticity of soil layers.

### 2.4.3. Geosynthetic reinforcement effects

Several parameters such as i) lateral restraint effect, ii) lateral confinement effect, iii) tension membrane effect, iv) limited depth effect, and v) wide slab effect of geosynthetic reinforcement etc., are responsible to enhance the bearing capacity of foundation soils. (Mandal and Sah, 1992) reported that the geosynthetic provided higher bearing capacity for soil foundation with a rigid base and with smaller depths. When a

load is applied, geosynthetic is deformed to develop tension, which has the uplift force i.e., the vertical component of resistance, known as tension membrane effect.

The increment of the bearing capacity due to reinforcement is often expressed by bearing capacity ratio (*BCR*) and determined by Equation – 2.6 (Binquet and Lee, 1975). As shown in (Figure 2.4 (b)),  a geosynthtic reinforced foundation soil provided higher bearing capacity as compared to unreinforced one, in case of plate laod testing.

$$BCR = \frac{q_{reinforced}}{q_{unreinforced}} \qquad \text{(Eq – 2.6)}$$
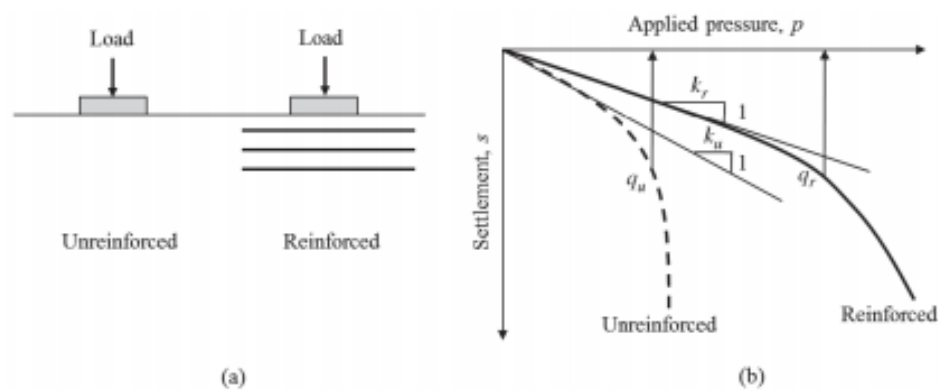


Figure 2.4: (a) Plate load tests on the reinforced and unreinforced foundations (b) settlement vs the applied pressure.

## 2.5. Geosynthetic reinforcement technique in previous studies

The use of geosynthetic materials such as geotextiles, geomembranes, and geocells are quite common in the geotechnical engineering application in order to improve the performance properties of problematic soils, however, the use of polythene sheeting in this respect is quite limited. There are several practical applications of geosynthetic to be used in the routine infrastructure development projects, including, canal lining, drainage protection, reinforcement of retaining walls, etc., but one of the most common uses of this material is to reinforce the weak foundation pad in

combination with other materials. Several studies have been conducted in this respect to examine the increase in the bearing capacity of soil using geosynthetic in foundations.

(Shin et al., 1993) worked on experimental models to examine the ultimate bearing capacity of saturated clay, strengthened with geogrid and concluded that the foundation provided maximum bearing capacity when the geogrid layer was placed at a depth of 1.8 x the width of footing and its width was 4.5 - 5 x the width of the footing. (Khing et al., 1994) conducted laboratory tests to examine the optimal thickness of the sand layer, underline by the week clay, strengthened with geogrid at the sand-clay interface, and reported that the foundation provided maximum ultimate bearing capacity when the thickness of sand layer was 2/3$^{rd}$ of footing width. Similarly, the depth and width of geogrid were 1.5 and 6 x the width of footing respectively.

(Tafreshi and Dawson, 2010) executed the bearing capacity of geosynthetic in combination with granular materials and clayey soils in foundations and reported that the bearing capacity was about 50% more for two layers of granular materials than that of one layer. Furthermore, the study concluded that the increase in strength was higher for geomembrane as compared to geocells. (Abu-Farsakh et al., 2013) executed laboratory tests to examine the influence of the number of reinforcement layers, tensile modulus, depth of reinforcement from the top, the spacing between layers, type of geosynthetic reinforcement, embedment depth, and shape of footing on bearing capacity of soils; and concluded that strain was reduced up to 20 percent, when two or more geosynthetic layers were used. (Cicek et al., 2015) focused on the length of geosynthetic rather than its thickness to enhance the bearing capacity of soft soil below the strip footing, and concluded that the BC increased with an increase in the length of reinforcement up to 2$B$, after then the strength remained constant.

(Zukri et al., 2017) performed experimental investigations using polyethylene terephthalate (PET) bottles and polypropylene (PP) fibres, in order to improve the engineering properties of clayey soil. The study reported that the bearing capacities of foundation soil were increased from 325 kN/m$^2$ to 367 kN/m$^2$ and 325 kN/m$^2$ to 365

kN/m$^2$ for PET and PP respectively, showing insignificant differences in strength, however, a major difference was noted in the optimal values, giving 10% and 20% by the weight of soil of PET and PP fibers, respectively.

(Ouria and Mahmoudi, 2018) examined the bearing capacity of strip footing for the cement-treated interface of sand and reinforcement (geocell and geotextile) and concluded that the bearing capacity of soil with a single layer of geotextile layer increased from 1.46 to 2.2 times to that of the unreinforced soil. Similarly, when the soil was reinforced with cement, it resulted in an increase in the BC from 1.71 to 2.31 times to that of the unreinforced one. Moreover, the bearing capacity of geocell or geogrid reinforced footings was observed to be 10-15% more than that of the bearing capacity of the footing reinforced with geotextile. (Zhou and Wen, 2008) performed physical modeling to examine the bearing capacity of sand, strengthening it with one and two layers of geosynthetics and concluded that the settlement was reduced up to 44% due to an improvement in the subgrade reaction coefficient ($K_{30}$) up to 3000% as a result of geosynthetic reinforcement.

## 2.6. Overview of Plaxis 2-D

The application of the numerical methods like finite difference code (H. Burd and Frydman, 1997) and finite element method (K. Lee et al., 1999; Chung and Cascante, 2007; Ornek et al., 2012) is quite common in geotechnical engineering to predict the soil behaviour in shallow foundations. The difference commercial codes such as ABACUS, FLAC-3D, and PLAXIS etc., are employed to execute to finite element studies in this regard. However, Plaxis 2D is mostly used due to its easiness, accuracy, and precision (Kenny and Andrawes, 1997).

### 2.6.1. Types of models

Plaxis can execute the soil behaviour, generating different models -i) linear elastic model, ii-) jointed rock model, iii-) hardening soil model, iv-) Mohr-Coulomb model, iii-) soft soil creep model and vi-) soft soil model for different conditions.

### 2.6.1.1. Linear elastic model (LE)

The linear elastic model applies Hooke's law to simulate the soil behavior, focusing on Poisson's ratio and Young's modulus. It is an initial model for simulating stiff material.

### 2.6.1.2. Hardening soil model (HS)

The hardening soil model simulates the soil behaviour, similar to that of the Mohr-Coulomb model, which only considers the limiting state variables including $\psi$, c, and $\varphi$ in the analysis. However, the hardening soil model in addition to above mentioned parameters, also uses oedometer loading stiffness ($E_{oed}$), the triaxial-unloading-stiffness ($E_{ur}$), and triaxial stiffness ($E_{50}$) as input parameters to examine the soil stiffness, more precisely.

### 2.6.1.3. Jointed rock model

The jointed rock model is an elasto-plastic model, which is used to simulate the behavior of fault directions and stratification rock layers, considering the anisotropic conditions.

### 2.6.1.4. Soft soil model (SS)

The soft soil model/cam clay model is employed to predict the behaviour of normally consolidated soils, incorporating the influences of primary compression in the analysis.

### 2.6.1.5. Soft soil creep model (SSC)

The soft soil creep model is most commonly employed to predict the hevaiour of normally consolidated silt and peat (Kuory et al., 2002). While simulation, the model considers the soil as creep soil as an input parameter.

### 2.6.1.6. Mohr-Coulomb model (MC)

Mohr-Coulomb model simulates the soil behaviour as a linear elastic perfectly-plastic model, using five input parameters such as c and φ for plasticity; ν and E for elasticity and ψ for dilatancy angle.

### 2.6.2. Features to simulate the soil behavior

Generally, Plaxis-2D simulates the soil behaviour for drained, undrained, and non-porous conditions, developing stress-strain relationships. The drained condition is applied in the model when there are no chances for the development of the pore water pressure within the soil mass and this condition prevails when the loading rate is slow, and the soil has high permeability; On the other hand, the undrained condition is applied in the model to simulate the behaviour of pore water pressure within the soil mass, and this condition prevails in soils of lower permeability (Craig, 1974). It is the property of the Plaxis to recognize the material properties, distinguishing between the total stress and effective stress conditions. According to (Gouw Dr, 2014), the model simulates the initial conditions of soil mass, considering its geometric configuration, groundwater conditions, and the initial stress state, initially, following a $K_0$ procedure in order to generate zero stress condition and full soil weight within the materials. The $K_0$ generates the soil body stresses by using Equation 2.7, proposed by (Fourie and Potts, 1989).

$$\sigma'_{h0} = K_0 \, \sigma'_{v0} \qquad\qquad (Eq-2.7)$$

Different boundary conditions such as side fixities, unit weight of different materials and ground water conditions etc., are also applied in the model to execute the analysis. The model has the potential to simulate the interface behaviour of two different materials such as geosynthetic and soil. For this purpose, an appropriate interface value ($R_{inter}$) is chosen for the roughness of the interaction, being used as a strength reduction factor. (M.A Sayed, 2012) examined the interface values for different foundation materials and reported some typical strength reduction factors, as shown in Table 2.6. In the modeling of the soil and polythene sheet in the plaxis-2D, the strength reduction

factor has a typical value of 0.85 (Brinkgreeve and Shen, 2011), and 1 means that there is complete contact between soil and the structural element.

Table 2.6: Strength reduction factors for different interface materials

| | |
|---|---|
| Interaction sand/steel | $= Rinter \approx 0.6 - 0.7$ |
| Interaction clay/steel | $= Rinter \approx 0.5$ |
| Interaction sand/concrete | $= Rinter \approx 1.0 - 0.8$ |
| Interaction clay/concrete | $= Rinter \approx 1.0 - 0.7$ |
| Interaction soil/geogrid (grouted body) (interface is not necessary) | $= Rinter \approx 1.0$ |

Plaxis is facilitated to generate two types of models, i) strain model (two dimensional) and ii) axisymmetric model (three dimensional). During data execution, the model has the tendency to generate either 12 stress points with 15 nodes triangular element or 3 stress points with 6-nodes triangular element as shown in Figure 2.5.
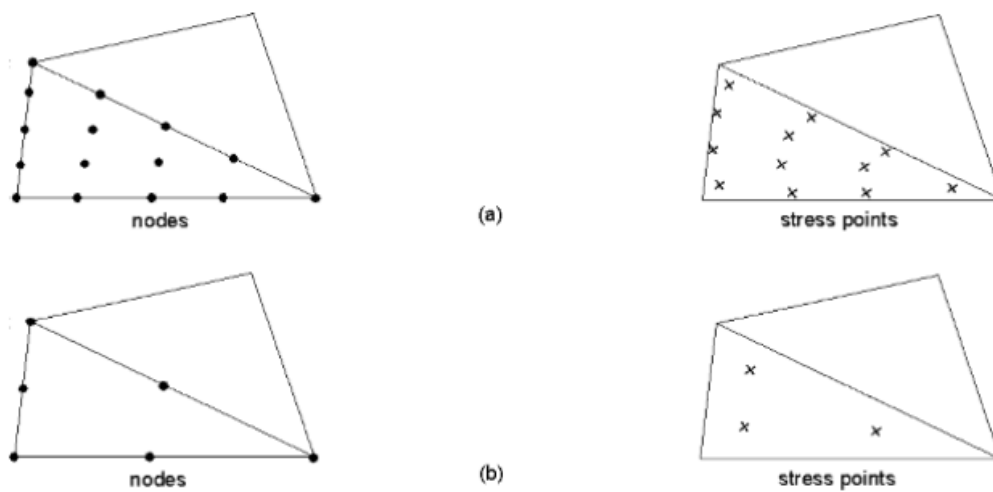


Figure 2.5: Element types in PLAXIS

The model divides the geometry into the triangular elements with different mesh densities, classifying it as coarse, medium, and fine meshes. (Ornek et al., 2012) reported that a fine meshing required more time for the analysis but alternately produced more accurate results. Plastic, safety ($\emptyset - c$) and consolidation analysis are facilitated in the model to do calculations, and the model applies a particular type of analysis, based on the soil behaviour as discussed in section 2.7.2. Plastic analysis is generally applied to

execute a total stress analysis, eliminating a need of pore water pressure – time relationship. (Kuory et al., 2002) suggested to use safety (ø – c) analysis when there is a need to determine the factor of safety , with a gradual reduction in friction angle and cohesion until the soil collapses, and this types involves a calculation phase to get the factor of safety. (Kuory et al., 2002) proposes that, when a soil undergoes volume changes, and excess pore pressure-time relationship is required precisely, then a consolidation analysis needs to be executed.

Furthermore, the model is facilitated to apply loading in stages to simulate existing and incremental stresses within the soil medium accurately, which include stage construction, total multipliers, and incremental multipliers. Stage construction is used to simulate initial stresses, based on the material properties and boundary constraints. The total multiplier is used to simulate the soil behaviour for external loading conditions whereas incremental multiplier is used to simulate the increments in the applied external loading conditions within the soil medium. Finally, stress distribution, the load-deformation curves, and failure patterns of foundation soils are plotted for design recommendations. According to (Kuory et al., 2002), the analyzed test data enabled to determine the value of any influential parameter at any point within the soil matrix.

# 3. MATERIALS AND METHOD OF THE TESTING PROGRAM

## 3.1. Introduction

In this chapter, testing of material properties like clay, granular material, and polythene plastic sheet is described. The method of preparation of the soft clay foundation bed and laboratory modeling setup is also described. In addition, all the numerical and physical testing program and testing procedure of the model to improve the soft soil is discussed.

## 3.2. Materials

The materials clay, sand, and polythene sheet were used in the research study to develop physical and numerical models in order to examine the BC of composite soil foundation. The sand was collected from Lawrencepur, located 64 km from the capital region Islamabad, Pakistan. The clayey soil used was got from Lodhran Punjab, Pakistan, which was selected on the presumption that the road constructed of this soil heaved after two years of construction due to seepage. Figure 3.1 shows the location point of the clayey soil. The polythene sheet was got from Lucky Plastic Industries (Pvt) Limited, Islamabad, Pakistan with thickness and density of 0.6mm and $0.960g/cm^3$ respectively.

Figure 3.1: Soil sample collection point at Lodhran, Punjab

## 3.3. Soil characterization

### 3.3.1. Grain size distribution

Sieve analysis was performed to examine the grain size distribution as per ASTM D 422-00 standard for both clayey soil and sand. Hydrometer analysis was carried out to categorize the soil, passing through # 200 sieve, following the procedure as discussed in ASTM D 422-63 standard. Moreover, a sieve shaker was used for sorting out the sand particles. Figure 3.2 shows a pictorial view of the hydrometer analysis performed in the laboratory.



Figure 3.2: Scheme of the hydrometer analysis in the laboratory

### 3.3.2. Atterberg limits

The liquid and plastic limits tests were executed following the guidelines as discussed in ASTM D423-54T and ASTM D424-54T standards respectively. These tests were performed on oven-dried samples passing through sieve # 40. Figure 3.3 shows the liquid limit test setup in the laboratory.



Figure 3.3**:** Liquid limit test arrangement in the laboratory

### 3.3.3. Moisture-density relationship

The standard Procter tests were performed to develop moisture–density relationships (compaction curves) of sand and clayey soil, following the guidelines as per ASTM D 698 – 00 standard (Figure 3.4.) As the moisture content increased beyond a certain limit, the clay adhered with the hammer and the mold during hammering. A knife with a flat and sharp edge was used to clean the adhered clay from the hammer and the mold.

Figure 3.4: Compaction test performed in the laboratory

### 3.3.4. Unconfined compressive strength

The unconfined compressive strength (UCS) of the clayey soil was figured out, performing the unconfined compressive tests according to the guidelines as discussed in ASTM D-2166 standard. Figure 3.5 shows an experimental set up of these tests. The samples with 80 mm height and 40 mm diameter (2:1) were prepared for the tests, following the criteria as discussed in the standard. Regarding the specimen dimensions of the soft soils for these tests, different criterions have already been discussed in Section 2.1. The tests were executed at the moisture-contents of 22%, 26%, 30% and 34% by weight. The replicate samples were prepared for each moisture content and then averaged the value. The samples were kept soaking for 5 days before the testing, keeping these in airtight plastic bags. According to (K. Lee et al., 1999), the soil samples were soaked for the uniformity of moisture throughout the sample.

While performing these tests, two problems were encountered: i-) the soil adhered with the mold during compaction due to its sticky behaviour and ii-) the samples were bulged during the application of loads, not providing the maximum shear stress, so the UCS was determined, referring to 10 percent of strain as reported in ASTM standard.

Figure 3.5: Scheme of unconfined compressive strength test

### 3.3.5. Portable vane shear

The portable vane shear (PVS) tests were executed to examine the undrained shear strength of clayey soil, following the guidelines as discussed in ASTM D-8121 standard. The specimens were prepared in CBR molds at 95 percent of the maximum dry density, applying 25 blows per layers and following the same guidelines as discussed in ASTM 1883-07. The samples were kept soaking for 5 days before the testing, keeping these in airtight plastic bags. Finally, the undrained shear strength and the moisture content relationships were developed. Figure 3.6 represents the soil specimens in the vane shear device.



Figure 3.6: Portable vane shear test

### 3.3.6. Direct shear

Direct shear tests were accomplished following the guidelines as per ASTM D-3080 to examine the drained shear strength of sand and undrained shear strength of clayey soil. The clay samples were compacted at 95 percent of $\gamma_{d\,(max)}$ at the 30 percent of $\omega$, for which the soft state existed (Yadu and Tripathi, 2013). Similarly, the sand samples were compacted at 95 percent of $\gamma_{d(max)}$ at 30 percent of $\omega$ as reported by (Bagherzadeh-Khalkhali and Mirghasemi, 2009). The soil specimens were sheared in the direct shear device, applying the normal stresses of 50 kPa, 100 kPa, and 200 kPa for drained and undrained conditions in the sand and the clay respectively. The clay sample was near to saturation at 30 percent moisture content and the load was applied so quickly, not allowing the water to drain out of the sample (Fredlund and Rahardjo, 1993). The samples were sheared at the rate of $5 \times 10^{-3}$ mm/sec in this study. The c and $\varphi$ parameters estimated from these tests were further used in Plaxis 2D as input data to model the bearing capacity of the footing.

### 3.3.7. Specific gravity

Specific gravity tests were performed as per the guideline of ASTM D 854-14 standard for both the clay and sand (Figure 3.7).



Figure 3.7: Pictorial views of specific gravity tests

### 3.3.8. Swelling

(Sridharan et al., 1986) reported that the swelling pressure, swelling potential, and free swell / swelling index was observed representative of the swelling behaviour of soil. So, in this study, the swelling pressure, swelling potential, and swelling index of the soil were determined to examine its swelling behavior. For the free swell or swelling index, the criteria as discussed by (Mohan and Goel, 1959) was followed. In this test, 10g of soil samples passing from sieve# 40 was poured into the 10 ml of distilled water and the kerosene oil too, separately. The soil samples were allowed to keep in water and kerosene oil for 24 hours and after then the final volume of the soil mixed with water and kerosene oil were recorded. Equation 3.1 was then used to define the free swelling index of the soil.

$$\text{Free swell index} = \frac{V_{dis} - V_{ker}}{V_{ker}} \text{ x } 100 \qquad (Eq-3.1)$$

Swelling tests were performed to determine one-dimensional wetting induced expansion for different pressures, following the guidelines as discussed in ASTM-4546-14 standard, using an odometer device. The swelling potential defines the amount of vertical expansion under the pressure of 1kPa (20lbf/ft2) and the swelling pressure is the minimum stress to stop the soil sample from expansion i.e., ($\varepsilon$=0).

In this test, the re-molded samples were held in the ring in the saturated condition under the vertical loads and a dial gauge was used to find out the variation in the sample thickness as shown in Figure 3.8. The sample is allowed to swell without pressure for up to 24 hours, and then loads of 12.5, 25, 50, and 100 kPa were added alternately until no distortion/expansion of the sample was seen. Finally, the relationships between the vertical strain and vertical pressure were drawn to estimate the swelling potential and swelling pressure (Equation 3.2)

$$Sp = \Delta h \text{ x } 100/h \qquad (Eq-3.2)$$

Figure 3.8: Odometer machine for swelling test

### 3.3.9. Activity

In this study, activity was determined to figure out the clay minerals like montmorillonite, illite, and kaolinite. The activity is defined as the ratio of the plastic index (P.I) to the percentage of clay size fraction (Skempton, 1953).

$$A = \frac{PI}{CF} \qquad\qquad (Eq - 3.3)$$

### 3.3.10. Maximum and minimum void ratio

The maximum and minimum void ratios of sand, were determined following the guidelines as per ASTM D 4253 standard. The clean sand was passed through #4 sieve, allowing it to fall under gravity into a calibrated mold through a funnel. The mold was weighed as filled, trimming off the excessive sand form its top, carefully. The maximum void ratio ($e_{max}$) of sand was then obtained in the loosest state. The loose sand in the same mold was covered with a surcharge plate and vibrated it on the vibrating table for 8 minutes. The surcharge plate was settled down due to the densification of the underneath sand, due to the table vibration. The settlement of the surcharge plate and the volume of the densified sand were noted to determine the minimum void ratio ($e_{min}$),

and then, Equation 3.4 was used to calculate the maximum and minimum dry unit weight from the minimum and maximum void ratio, respectively.

$$\gamma_{d\,(min,\,max)} = \frac{G_s\,Y_\omega}{1+e_{(max,min)}} \qquad\qquad (Eq - 3.4)$$

In this study, sand used in the physical model was categorized as medium dense, based on its relative density. The $D_r$ of sand for different degrees of compactness are shown in Table 2.5, and medium dense sand shows a relative density of 35-65 percent. As suggested by (Tavangar and Shooshpasha, 2016), a relative density of 55 percent was used in the current study to develop the physical model. Based on the relative density ($D_r$) and maximum unit weights $\gamma_{d\,(max)}$ and minimum unit weights $\gamma_{d\,(min)}$, the in situ dry unit weight ($\gamma_d$) of sand was calculated using Equation 3.5. The weight of sand, compacted to a known volume in the physical model tank was then calculated from the dry unit weight.

$$D_r = \frac{Y_d - Y_{d(min)}}{Y_{d\,(max)} - Y_{d\,(min)}} \; x \; \frac{Y_{d\,(max)}}{Y_d} \qquad\qquad (Eq - 3.5)$$



Figure 3.9: Pictorial view of the arrangement of equipment for the determination of $e_{max}$ and $e_{min}$.

## 3.4. Polythene sheet characterization

### 3.4.1. Tensile strength

A Universal Testing   Machine (UTM) (SHIMAZDU) was used to examine the tensile strength of the polythene sheet at the School of Chemical and Material Engineering (SCME), NUST, Pakistan. The procedure as discussed in ASTM D638-14 was followed to perform these tests. Figure 3.10 shows some pictorial views of the experimental scheme in the laboratory, and Table  3.1 shows the specifications of the UTM used for testing.

Table 3.1**:** Universal testing machine specifications

| Specification | Value |
|---|---|
| Strain Rate | 0.0005 – 1000 mm/min |
| Max Force | 20 kN |
| Max thickness of grip section | 7 mm (Flat sample) |
| Max Width of the grip section | 24 m (Flat sample) |



Figure 3.10**:** Pictorial views of the specimen preparation and arrangement of the tensile test of the polythene sheet

## 3.5. Laboratory model testing program

The small scale physical model tests were developed in the laboratory of geotechnical engineering at the Department of Civil Engineering, NUST, Islamabad.

### 3.5.1 Test box and components

A physical model was established to examine the bearing capacity of the polythene-reinforced foundation which consisted of a loading beam and a steel box. The length, width, and height of the model box were 760 mm, 760 mm, and 600 mm respectively. The loading frame with height 1200 mm and width 900 mm was supplemented with the steel box. A square rigid steel plate of 152.4 mm x 152.4 mm x 10 mm was used to transmit the load from the hand-operated hydraulic jack to the foundation (Figure 3.11).



Figure 3.11: View of small-scale loading beam and steel box

A loading beam was manufactured and designed to apply the continuous load at the footing in the model. A calibrated proving ring was placed between the reaction frame and the stroke of the hydraulic jack to determine the applied load. Linear variable displacement transducers (LVDT) were placed on the footing in vertical alignment, to eliminate the chances of errors in the measurement. These LVDT were attached to the digital inverter to measure the settlement (Figure 3.12).



Figure 3.12**:** Schematic view of the physical model setup of load and displacement

### 3.5.2. Scheme of the model testing

Figure 3.13 shows a scheme of the physical model developed in the geotechnical laboratory at the Department of Civil Engineering, NUST, Pakistan. Equation 3.6 as proposed by (Latha and Somwanshi, 2009) and (Kolay et al., 2013) was used to estimate the effective depth of the polythene (*d*) from the footing base.

$$d = u + (N\text{-}1) \, x \, h \hspace{3cm} (Eq-3.6)$$

In Equation 3.6, $N$ = the number of polythene layers used, $h$ = consecutive vertical in-between spacing of polythene sheets and $u = 1^{st}$ layer location, calculated from the model footing base.
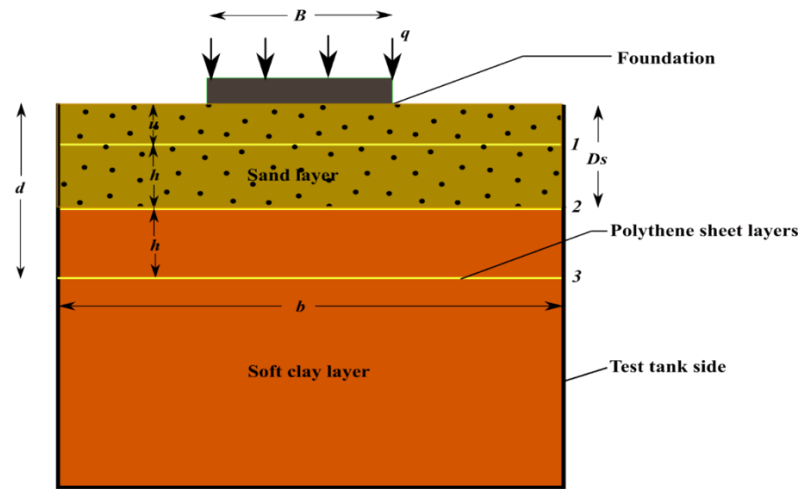
Figure 3.13: General scheme of the physical model

The magnitude of *BCR* for the given footing of width depends upon non-dimensional parameters in terms of footing width (*B*) such as; top layer spacing to footing width (*u/B*), the spacing between two consecutive layers to footing width (*h/B*), effective depth of reinforcement to footing width (*d/B*), and length of reinforcement to footing width (*b/B*). (Mandal and Sah, 1992; Demir et al., 2008) performed BC tests on the geogrid reinforced clay foundation and founded that maximum reduction in settlement occurred at *u/B* = 0.25 with one geogrid layer. (Latha and Somwanshi, 2009) reported that a maximum increase in *BCR* of square footing was noticed for *h/B* = 0.5 and *b/B* = 4 –5.93, for three layers of geogrid and geotextile, separately. (Hasanzadeh and Choobbasti, 2016) suggested that the maximum strength in the bearing capacity occured for the depth of replacement to footing width (*Ds/B*) of 0.7 – 0.8.

Table 3.2. Different tests and parameters used in the physical model testing

| S. No. | Description | Ds/B | u/B | h/B | d/B | b/B | N |
|--------|-------------|------|-----|-----|-----|-----|---|
| 1 | only soft clay | …. | …. | …. | …. | …. | …. |
| 2 | Sand overlying soft clay | 0.75 | …. | …. | …. | …. | …. |
| 3 | 1 polythene sheet in the sand layer above soft clay | 0.75 | 0.25 | …. | 0.25 | 5.00 | 1.00 |
| 4 | 1 polythene sheet in the interface of sand and soft clay and 1 in the sand layer | 0.75 | 0.25 | 0.50 | 0.75 | 5.00 | 2.00 |
| 5 | 1 polythene sheet in soft clay, 1 in the interface of soft clay and sand and 1 in the sand layer | 0.75 | 0.25 | 0.50 | 1.25 | 5.00 | 3.00 |
| 6 | 2 polythene sheets in the soft clay, 1 in the interface of soft clay and sand and 1 in the sand | 0.75 | 0.25 | 0.50 | 1.75 | 5.00 | 4.00 |
| 7 | 3 polythene sheets in the soft clay, 1 in the interface of sand and soft clay and 1 in the sand | 0.75 | 0.25 | 0.50 | 2.25 | 5.00 | 5.00 |

Initially, the scheme of the alternate layers in the foundation was set as: i-) $u/B$ = 0.25, ii-) $h/B$ = 0.50, iii-) $b/B$ = 5 and iv-) $Ds/B$ = 0.75. Table 3.2 shows a scheme of different materials arrangements, being used in the model. Two series of physical model tests were executed in the laboratory; i-) a series of tests in which only soft clay was tested, ii-) a series of tests in which different number of layers of polythene sheet ($N$) were placed in the composite zone while the optimum fill thickness of sand was kept constant as 0.75B.

### 3.5.3. Scale effect

The idea of the scale effect was presented by (Berry, 1935) and stated that the BC of dense sand foundation with constant relative density increased with an increase in footing dimensions. The study concluded that the footing size was more dependent

upon the scale effect rather than the frictional angle ($\varphi$) of the granular materials. (T. Tatsuoka, 1991) and (F. Tatsuoka, 1994) concluded that two factors were mainly observed responsible to influence the scale effect of footing dimension, i-) the dependency of the stress level on the mechanical properties of the sand and ii-) the particle size effect; which alternately influenced the BC of the foundation soil, and furthermore, (T. Tatsuoka, 1991) and (Siddiquee, 1991) employed centrifuge and numerical simulation approaches to examine the scale effect for these parameters.

Other researchers such as (Ovesen, 1975; Bolton and Lau, 1989; Herle, 1997) also conducted investigations to examine the effect of particle size effect ($B/d_{50}$) to define its suitable range. The studies reported that there was no effect of the particle size in the case of $B/d_{50} > 50\text{-}100$. In the current study, to eliminate the scaling effect, a footing width of 152.4 mm with smaller particles size of 0.3 mm in relation to $d_{50}$ (Figure 4.1) was used to get an acceptable ratio of $B/d_{50} > 100$.

(Bransby and Smith, 1975) suggested to use a relatively larger tank with frictionless sides to eliminate the influence of scale effect on the bearing capacity of laboratory tests. So, the inside of the laboratory model tank and walls is oiled to decrease the roughness between tank and foundation materials, and the length and width of the tank are taken as $5B$ with thickness of the soil layer of $4B$. Steel angles are provided on the sides and top of the model tank to stop the lateral movement and to make it rigid. (Cerato and Lutenegger, 2007) suggested that the small scale physical model can be applied in the full scale model, if the sand in the small scale laboratory test is comparatively be in the looser state to that of the sand in the full-scale model state.

### 3.5.4. Preparation of model test

The volume of every layer was measured based on the dimensions of the model tank. According to the dry unit weight of 14.25 kN/m$^3$, the amount of silty clay was calculated for each layer. The clay sample was pulverized with the hammer and prepared by the hand mixing with 30 percent of the water as determined by PVS and UCS tests, and then transferred to the model tank, compacting in respective layers. The thickness

of each layer was changed from 75 mm to 100 mm, depending on the spacing between each reinforcement. Before putting the soft soil in the steel box, the grease oil was spread to the internal surface of the model tank to control the roughness and erosion.

The weight of the sand was found out based on the box volume and the dry unit weight (15.8 kN/m$^3$) which was calculated from the relative density of sand, using Equation 3.5. The relative density was assessed 55 percent in this study as suggested by (Tavangar and Shooshpasha, 2016), as the sand fell in the category of medium compactness. The calculated sand was mixed with the water content of 13 percent, obtained from the SPT, and then transferred to the model tank. There were the chances of lower layers in the tank to be compacted repeatedly, during the above layer compaction. In order to avoid this problem, the depth of the lower layers was set higher than that of the normal depth and the criteria as discussed by (Ladd, 1978) was followed in this regard. A 20 lb hammer falling from a height of 12 inches was used to compact the respective layers. The relative compaction of the sand in the small scale model was found out using Equation 3.7 as proposed by (K. L. Lee and Singh, 1971).

$$R_c = 80 + 0.2 \text{ x } D_r \,(\%) \hspace{3cm} (Eq - 3.7)$$

The soil was filled in the tank up to a total height of 600 mm. To ensure the uniformity of moisture, the test tank was covered with the polythene sheet for 05 days at room temperature to get the uniformity of moisture content (K. Lee et al., 1999). Plate load tests were carried out for a footing settlement up to 20 percent of the footing dimension, i.e., 30 mm in this study (Binquet and Lee, 1975). Furthermore, the tests were performed within 5 minutes to fulfil the criteria of undrained condition as suggested by (K. Lee et al., 1999). Figure 3.13 shows few pictorial views for the preparation of the clay and polythene layering in the soft soil.

The current research reports four alternative methods to estimate the ultimate bearing capacity from the bearing capacity and settlement relationships. Each method is unique and provides different values of the ultimate bearing capacity. However, (Lutenegger and Adams, 1998) and (Cerato and Lutenegger, 2007) set the priorities of

these methods in the following order as log method < tangent intersection method < 10 percent of settlement/footing width < hyperbolic method on the basis of data accuracy. However, (Sharma et al., 2009; Kolay et al., 2013) suggested modifications to the above mentioned criteria and reported that both, 10 percent of *s/B* and tangent intersection method provided the same UBC from the load settlement relationships. So, in this study, both of these methods were used to predict the ultimate bearing capacity.



Figure 3.14: View of soft clay preparation and layout of the polythene sheet

## 3.6. Numerical model testing program

### 3.6.1. Research methodology of FEM

The clay was brought about 600 km away from the experimental site. Therefore, seven tests were performed in the laboratory due to time constrain and larger quantity of clay, needed for each test. These physical model tests were executed to validate the numerical simulation tests, conducted under similar laboratory conditions, similar to that of (Abu-Farsakh et al., 2013). After validating the model, several combinations of parameters including; i-) effect of number of polythene layers (*N)*, ii-) effect of thickness of sand replaced overlying soft clay (*Ds*) iii-) effect of top 1st layer of polythene spacing (*u*), iv-) effect of in-between spacing of polythene (*h*) v-) effect of the length of the

polythene (*b*), vi-) the effective depth of the polythene layers (*d*) was tested using numerical simulation.

In total, 47 tests were executed for two types of conditions i-) soft clay reinforced with polythene sheeting, ii-) soft clay strengthened with polythene reinforcements and granular materials. Tables 3.3 and 3.4  represent the scheme of the test methodology for numerical simulation.

Table 3.3**:** Test methodology of soft clay reinforced with polythene

| S.No | Model type | Parameters | | Tests |
| --- | --- | --- | --- | --- |
| | | Constant | Variable | |
| 1 | only soft clay | | | 1 |
| 2 | Effect of top layer spacing | $b/B=5$, $N=1$ | $u/B=$0.13, 0.25, 0.33, 0.50, 0.63, 0.75, 1.00 | 7 |
| 3 | Effect of number of reinforcement layer | $b/B=5$, $u/B=0.25$ $h/B=0.50$ | $N=$1, 2, 3, 4, 5 | 5 |
| 4 | Effect of vertical spacing of the layer | $b/B=5$, $u/B = 0.25$, $N=3$ | $h/B=$0.25, 0.50, 0.75 | 3 |
| 5 | Effect of length of the reinforcement | $b/B=5$, $u/B=0.25$, $N=3$ | $b/B=$1, 2, 3, 4, 5 | 5 |
| | | | Total | 21 |

Table 3.4: Test methodology of soft clay reinforced with polythene and granular fills

| S.No | Model type | Parameter | | Tests |
| | | Constant | Variable | |
| --- | --- | --- | --- | --- |
| 1 | only soft clay | | | 1 |
| 2 | Soft clay replaced by the Sand | | $Ds/B$=0.33, 0.50, 0.67, 0.75, 1.00 | 5 |
| 3 | Effect of top layer spacing | $Ds/B$=0.75, $b/B$=5, $N$=1 | $u/B$=0.13, 0.25, 0.33, 0.50, 0.63, 0.75, 1.00 | 7 |
| 4 | Effect of number of reinforcement layer | $Ds/B$=0.75, $b/B$=5, $u/B$=0.25 $h/B$ = 0.50 | $N$=1, 2, 3, 4, 5 | 5 |
| 5 | Effect of vertical spacing of the layer | $Ds/B$=0.75, $b/B$=5, $u/B$=0.25, $N$=3 | $h/B$=0.25, 0.50, 0.75 | 3 |
| 6 | Effect of length of the reinforcement | $Ds/B$=0.75, $h/B$=0.50, $u/B$=0.25, $N$=3 | $b/B$=1, 2, 3, 4, 5 | 5 |
| | | | Total | 26 |

## 3.6.2. Plaxis 2-D

A finite element model (Plaxis 2-D) is most commonly employed as a commercial tool to carry out the stability and deformation analysis for many applications in geotechnical engineering. Different researchers like (Frydman and Burd, 1997; Chung and Cascante, 2007; Ornek et al., 2012; Vilas and Moniuddin, 2015) recommended to use Plaxis 2-D for BC simulation of shallow foundations. (Brinkgreve, 2002) reported that the tool proved an effective too to simulate, both the plane-strain and axisymmetric conditions. In this study, Plaxis was utilized to examine the bearing capacity of the composite shallow foundation.

## 3.6.2.1 General setting

In this study, the general setting of the Plaxis was included a plane strain, elastoplastic analysis, 12 stress points with 15 nodes element. The 15 nodded triangular elements produced higher quality stress and deformation results as compared to 6 nodded triangular elements, due to the presence of a larger number of stress points (Mosallanezhad and Moayedi, 2017).

### 3.6.2.2 Material set properties

After creating the geometrical model using points, lines, and footing elements, material set properties were assigned to the respective clusters and footing elements. The material properties of clay, sand, footing and polythene sheet are discussed as;

### 3.6.2.2.1 Soil

Mohr Coulomb's elastic perfectly plastic soil model was used to model the foundation soils to simulate the behavior of footing supported on composite soils. The sand and soft clay were modeled as a Mohr-Coulomb-drained material (Mosallanezhad and Moayedi, 2017) and a Mohr-Coulomb-undrained material (Vilas and Moniuddin, 2015; Al-Taie et al., 2016), respectively. The Mohr-Coulomb uses five input basic parameters to describe the stress state failure, i.e., E and $v$ for the elasticity, c, and $\phi$ for the plasticity and dilatancy angle ($\Psi$) for the volumetric strain (Ornek et al., 2012).

The properties of soft clay and sand used in the model are estimated from the laboratory tests, and are illustrated in Table 3.5. The unsaturated unit weight ($\gamma_{unsat}$) of the soil was figured out from the standard proctor test and saturated unit weight ($\gamma_{sat}$), using Equation 3.8 (Das, 2013).

$$\gamma_{sat} = (1 - \frac{1}{Gs}) \gamma_d + \gamma_\omega \qquad (Eq - 3.8)$$

Modulus of elasticity (E) of the silty clay was obtained from Equation 3.9, proposed by (El-kasaby, 1991). The $\beta$ for the clay with plasticity index greater than 20 varied from 100 to 500 (Duncan and Buchignani, 1976; Bowles, 1996). However, in this study, the E of sand was directly used as reported by (K. Lee et al., 1999) for the Mumbra sand because this particular sand gave almost the same index properties as Lawrencepur sand.

$$E = \beta \text{ x } C_u \qquad (Eq - 3.9)$$

Poisson's ratio (*v*) of clay was determined from the UCS tests and Poisson's ratio (*v*) of sand was calculated by using Equation 3.10, as proposed by (Trautmann et al., 1987).

$$v = 0.1 + 0.3 \left(\frac{\phi - 25^\circ}{20^\circ}\right) \qquad \text{(Eq – 3.10)}$$

The Dilatancy angle was calculated from Equation 3.11 (Osman and Bolton, 2005), showing a dilatancy angle equal to zero for the friction angle (ϕ) less than 30º. A positive dilatancy angle was implied in the drained condition which represented the dilation of sand in the shear conditions (Plaxis V8.2 manual, 2002).

$$\Psi = \phi - 30 \qquad \text{(Eq – 3.11)}$$

### 3.6.2.2.2. Footing plate and polythene sheet

The polythene sheet reinforcement was modeled considering it as an elastoplastic material, utilizing its material properties such as the axial normal stiffness and ultimate tensile strength per unit width (kN/m) for the analysis. (Belal et al., 2015) reported that Plaxis modeled the structural elements such as footing, considering it as a linear elastic model. The parameters including axial rigidity (EA), flexural rigidity (EI), unit weight per unit length (w), and Poisson's ratio (*v*) are required for the linear elastic model. EA and EI depend upon elastic modulus of the material (E) and thickness of the structure (d), which can be estimated from Equations 3.12 and 3.13, respectively (Dennis, 2006).

$$EA = E\,d \qquad \text{(Eq – 3.12)}$$

$$EI = \frac{E\,d^3}{12} \qquad \text{(Eq – 3.13)}$$

In the study, the properties of the footing were used as suggested by (Belal et al., 2015) and polythene sheet properties were obtained from the laboratory tests. The properties of the footing and polythene sheet are enlisted in Table 3.6.

Table 3.5**:** Properties of the foundation soil used in the numerical modeling

| S. No. | Properties | Clay | Sand | unit |
|---|---|---|---|---|
| 1 | Material model | Mohr coulomb | Mohr coulomb | |
| 2 | Material type | Undrained | Drained | ___ |
| 3 | Saturated unit weight of soil [$\gamma_{sat}$] | 19 | 21 | kN/m$^3$ |
| 4 | Unsaturated unit weight of soil [$\gamma_{unsat}$] | 17.75 | 19.5 | kN/m$^3$ |
| 5 | Cohesion [C] | 21 | 1 | kN/m$^2$ |
| 6 | Dilatancy angle [$\Psi$] | 0 | 12 | Degrees |
| 7 | Friction angle [$\phi$] | 5 | 42 | Degrees |
| 8 | Poisson ratio [$v$] | 0.45 | 0.35 | |
| 9 | Young's modulus [E] | 6500 | 13000 | kN/m$^2$ |

Table 3.6**:** Properties of the footing and polythene sheet used in the numerical modeling

| S.No. | Description | Steel plate | Polythene sheet | Unit |
|---|---|---|---|---|
| 1 | Modulus of elasticity [E] | 2E+8 | 107E+3 | kN/m$^2$ |
| 2 | Thickness [d] | 10 | 0.6 | mm |
| 3 | Weight per unit length [w] | 5.8E-2 | ___ | kN/m/m |
| 4 | Axial normal stiffness [EA] | 2E+7 | 64.42 | kN/m |
| 5 | Bending stiffness [EI] | 16.67 | 1.92E-6 | kN.m$^2$/m |
| 6 | Tensile strength [Np] | ___ | 4.2 | kN/m |

### 3.6.2.3. Interface and boundary conditions

It is essential to select a proper strength reduction factor ($R_{inter}$) to simulate the roughness at the interaction of steel, polythene sheet, sand, and clay in the model. (Brinkgreeve and Shen, 2011) suggested to use strength reduction factor of 0.6 and 0.5 at the interface of the sand and steel plate footing, and clay and steel plate footing respectively. However, in case of complete contact of soil with the reinforcement under normal pressure, (Gouw Dr, 2014) suggested to use $R_{inter}= 1$, considering it a rigid interaction. In the present study, the authors used $R_{inter}= 1$, considering a rigid interaction

between soil and the polythene sheeting. Few boundary conditions were also assumed to do the analysis. The total fixities were applied to constrain left and right sides, and the bottom and the top were left vertically free, as discussed by (Hasanzadeh and Choobbasti, 2016). The groundwater table was not considered in the analysis, and the gravitational constant was taken as 9.81 m/sec$^2$.

### 3.6.2.4. Mesh generation

(Demir et al., 2008) reported that the number of elements (mesh size) and nodes influenced the model output, significantly. After assigning the defined material properties to all the clusters (the geometry line's enclosed area) and structural elements, the mesh was generated by entering into a mesh generation setting. For this study, a very fine mesh in each cluster was selected, considering the accuracy of the test data.

### 3.6.2.5. Initial stress condition

The initial stress condition was applied after creating geometry and generating meshing in the model. In this study, $\sum$M-weight was kept equal to 1 so that the full weight of soil could be utilized to generate the initial stresses and to accept the default suggested value of $K_0$, as suggested by (Ornek et al., 2012). $\sum$M-weight represents an additional component in the model to simulate the self-weight of the material.

### 3.6.2.6. Calculation

The calculation steps started after applying the meshing and initial conditions. The loading type used in the calculation was the staged construction, in which the load was assigned in stages such as; in the first stage, a plate and positive interface was assigned to the construction element and in the second stage, prescribed displacements were assigned to the construction element.

It is required by the user to specify some of the control parameters, used in the calculation phases which may influence the test data within a certain phase. In this study, these control parameters were reset as i) displacement to zero, ii-) ignore undrained behavior, and    iii-) delete intermediate steps.

### 3.6.2.7. Output and curves

After the calculation stage, the output program provided an exaggerated deformed shape of the model, showing some suitable scale factors. The auto scale was selected in this step which scaled up the deformed mesh as per displacement of the footing and also accepted the scale factor value as suggested by Plaxis. Finally, the load-displacement curves were generated from the analysis.

# 4. RESULT AND DISCUSSION

## 4.1. Introduction

This chapter reports the results and discussions for both physical and numerical simulation test data, highlighting the effects of influential factors including, the spacing of top layer ($u$), in-between spacing of layers ($h$), the optimum total layers ($N$) and the optimum length of the polythene sheet ($b$) on the bearing capacity of soft soil foundations, strengthened with polythene reinforcement and granular materials.

## 4.2. Clay characterization

### 4.2.1 Grain size distribution

The grain size distribution of the silty clay and Lawerancepur sand are shown in Figure 4.1. The clayey soil showed smilar behaviour to that of Rariton clay (N. J.). The coefficient of uniformity (Cu) and coefficient of curvature (Cc) of sand is estimated to be 1.72 and 1.16 respectively, classifying it as a poorly graded granular materials (Das, 2013)
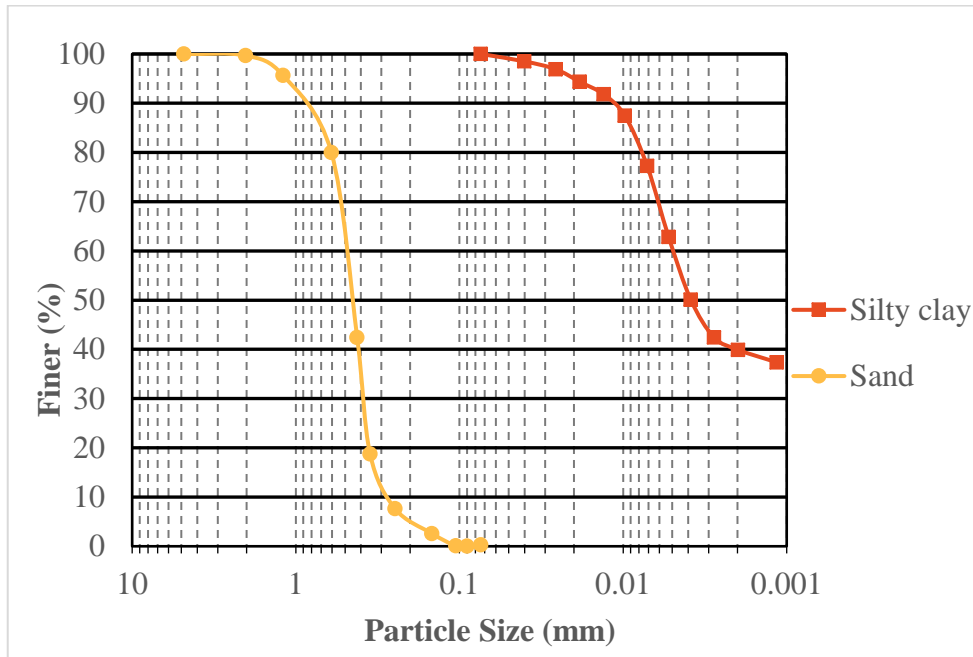
Figure 4.1: Particle size distribution curves for the sand and the clay soils.

### 4.2.2. Atterberg limits

The clayey soil shows liquid and plastic limits of 42 percent and 19.5 percent respectively, with a plasticity index of 22.5 (Figure 4.2). As per USCS and AASHTO system, the clayey sample falls in the category of low plastic silty clay (CL) and A-7-6 (23) respectively. Figures 4.3 and 4.4 show USCS and AASHTO soil classification systems for the plasticity index, respectively. The consistency Index ($I_c$) of silty clay is estimated 45 percent, validating its soft soil behaviour . According to ((Kempfert and Gebreselassie, 2006), a soil behaved as a soft soil, showing consistency index of $< 75\%$.
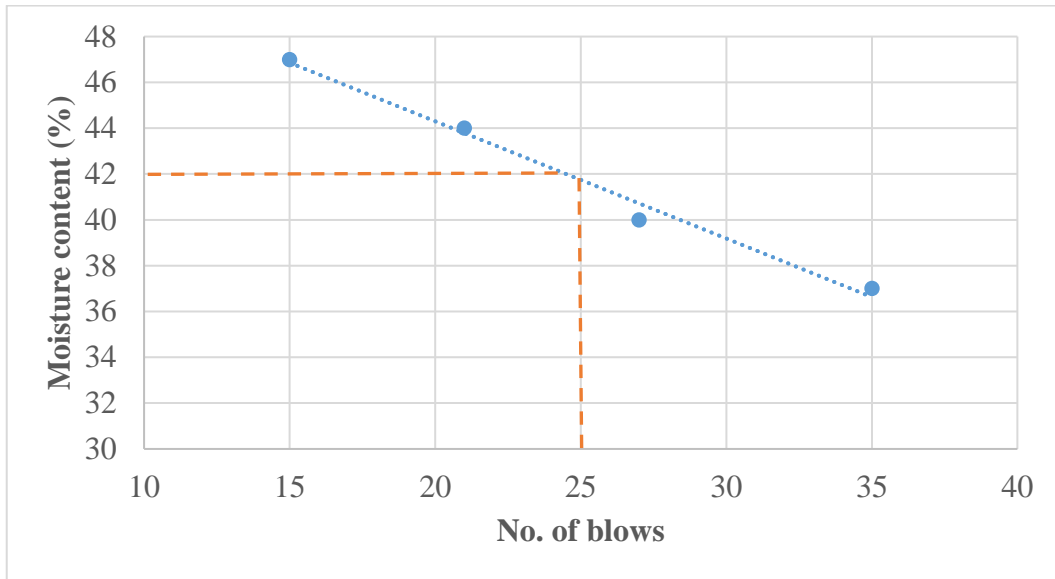
Figure 4.2: Liquid limit test results of the clay
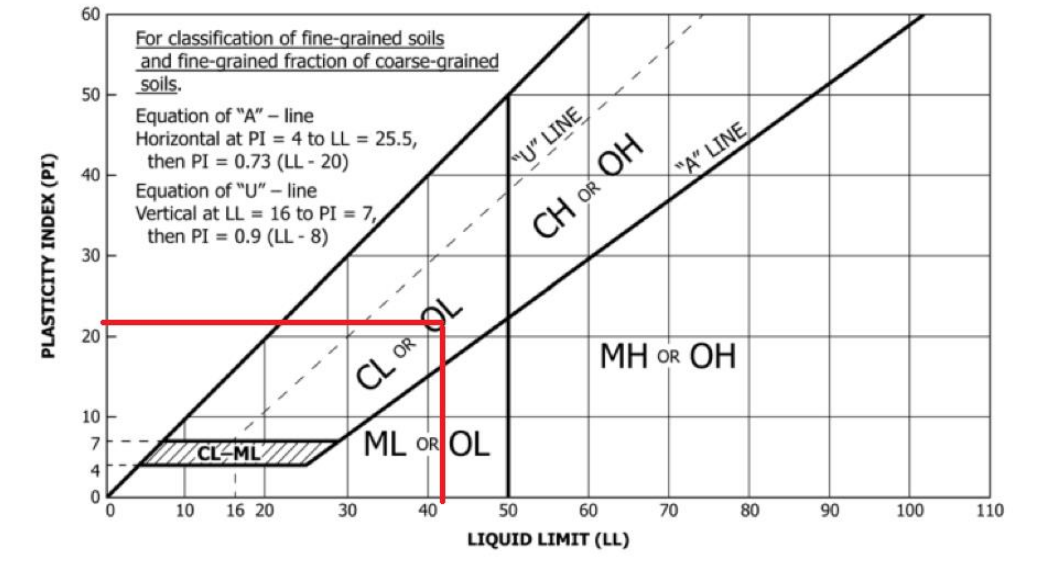


Figure 4.3: USCS classification - A line Chart
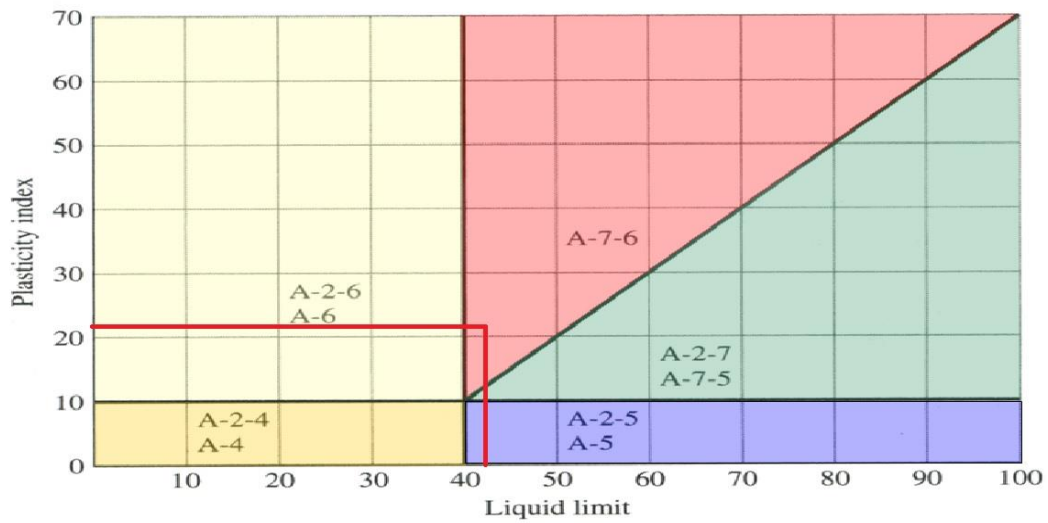
Figure 4.4: AASHTO classification chart

### 4.2.3. Moisture-density relationship

The moisture–density relationships are presented in Figures 4.5 and 4.6 of silty clay and sand respectively. The silty clay and sand gives maximum dry unit weights of 14.25 kN/m$^3$ and 16.75 kN/m$^3$ at the optimum moisture contents of 23 percent and 13 percent respectively.

### 4.2.4. Unconfined compressive strength

The variation in UCS values with different moisture contents of clay is shown in Figure 4.7. The UCS of clay decreases significantly from 140 kPa to 10 kPa with an increase in the moisture content from 22 percent to 34 percent respectively. Strength is taken corresponding to 10 percent of strain because molds bulge during testing. As discussed in section 2.1 (Terzaghi and Peck, 1967) reported that the clay behaved soft in nature at the specific moisture contents, providing unconfined strength between 12 and 50 kPa. As in Figure 4.7, the silty clay behaves as a soft soil for moisture contents between 27 and 33 percent.
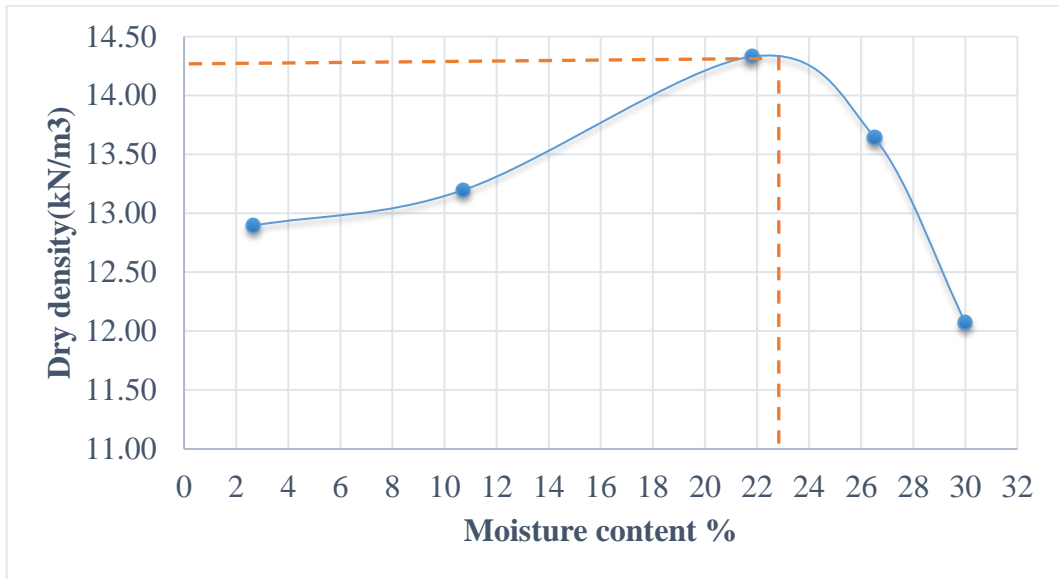
Figure 4.5: Moisture-density relationship of clay
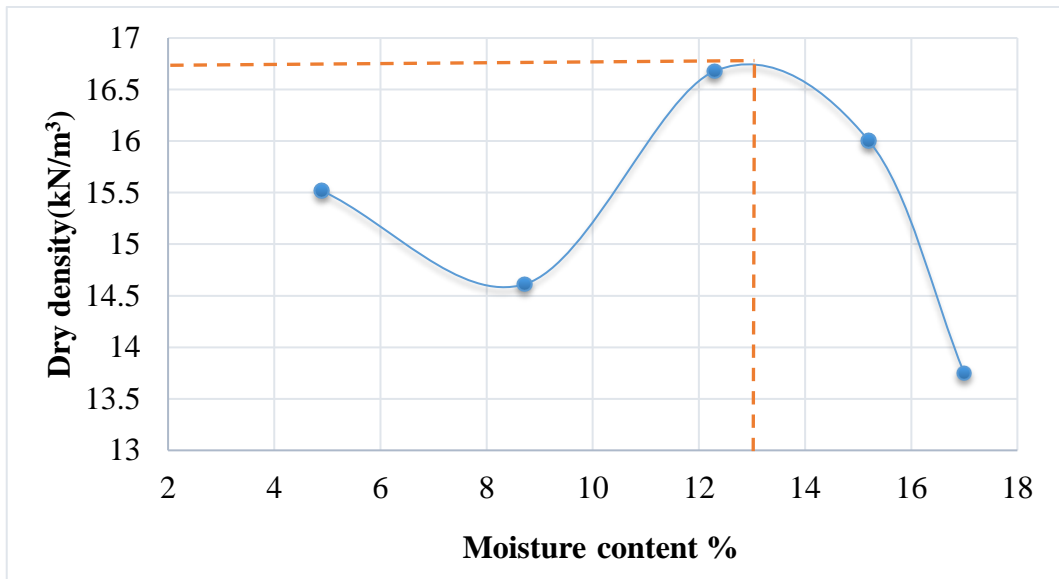


Figure 4.6: Moisture-density relationship of sand
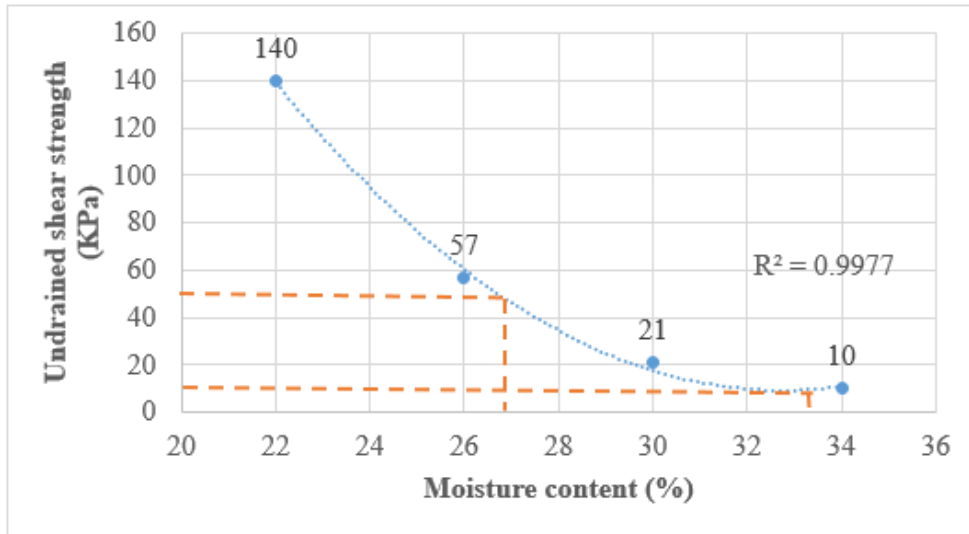
Figure 4.7: undrained shear strength-moisture content relationship

### 4.2.5. Portable vane shear

The variation in the magnitude of undrained shear strength with changes in the moisture content of the clayey soil are shown in Figure 4.8, and the soil behaves as a soft clay for moisture contents between 27.5 and 33.5. From the test data of unconfined compressive and portable vane shear tests, 30 percent of water content is selected for the preparation of the soft clay in the development of small-scale physical models.
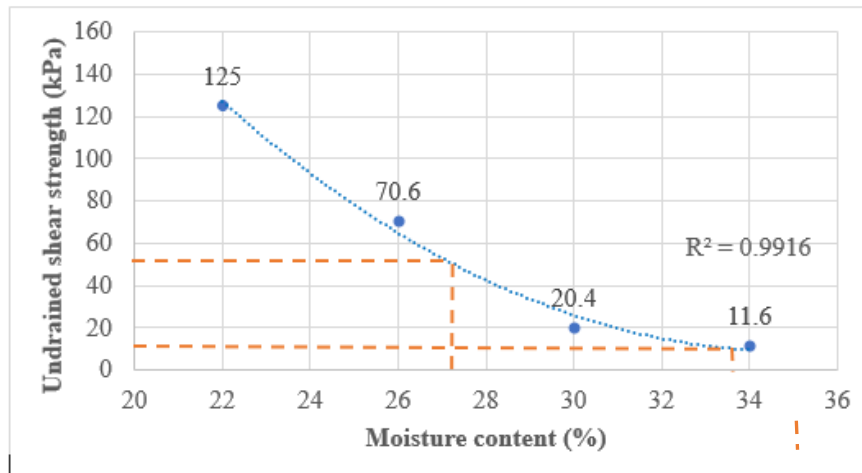


Figure 4.8: Portable vane shear test result

## 4.2.6. Direct shear

The silty clay at the soft condition shows cohesion of 21.167 kPa and friction angle of 5.0º (Figure 4.9). As in Figure 4.10, sand is a cohesionless material, giving an angle of internal friction of 42.0º.
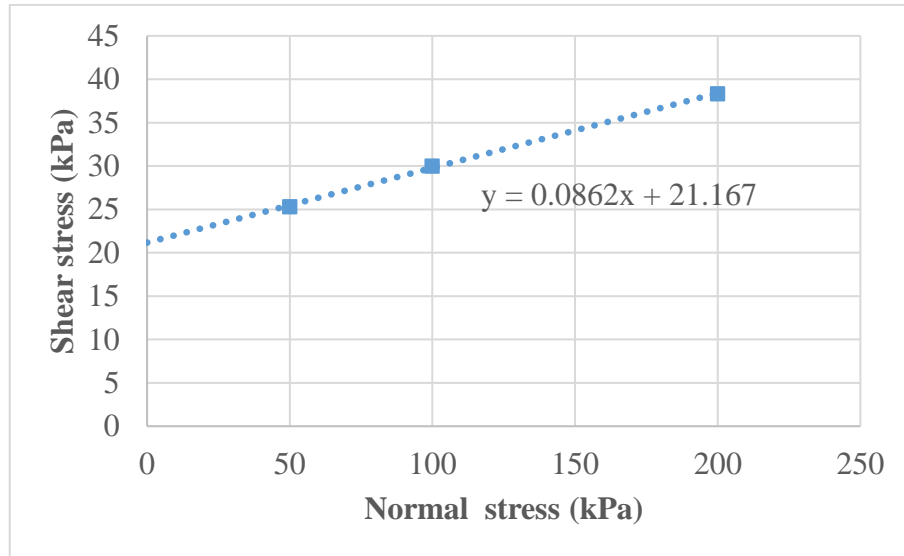


Figure 4.9**:** Shear stress and normal stress relationship of silty clay for direct shear test
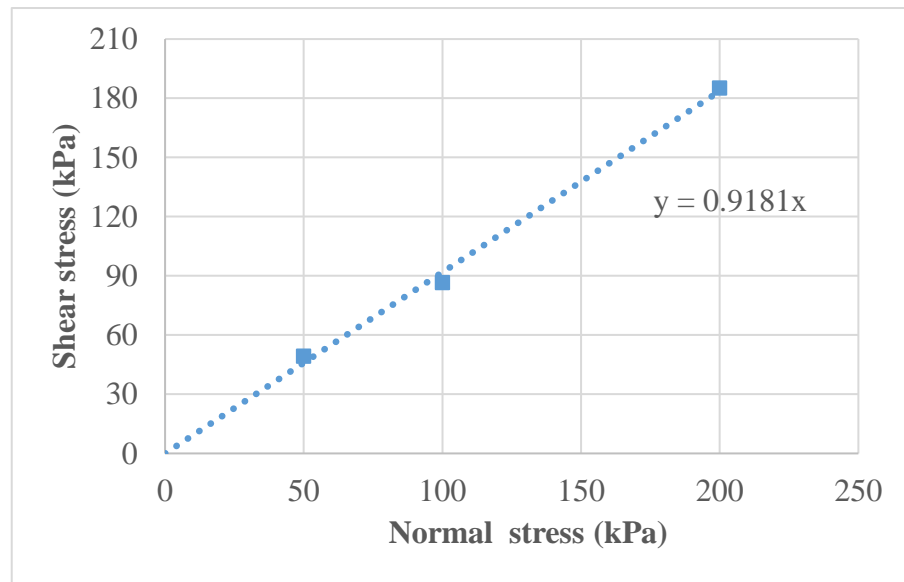


Figure 4.10**:** Normal stress and shear stress relationships of sand for direct shear test

### 4.2.7. Specific gravity

The specific gravity is estimated to be 2.56 of the silty clay and 2.66 of the sand.

### 4.2.8. Swelling

The free swell or swelling index of the clay is found to be 56 percent. It means that the silty clay has a medium degree of expansion, showing a marginal degree of severity as per Table 2.2 (Mohan and Goel, 1959). As shown in Figure 4.11, the soil shows a nonlinear swelling behavior with the rise of normal stress. Initially, the clay samples show swelling expansion with time for no load and after a certain time, the expansion becomes constant, reaching a maximum value of 4.66 percent of the swell strain. The percent swell of the sample deceases with a gradual increase in the stresses, which consequently provides -4.06 percent swell strain at maximum normal stress of 100 kPa. Figure 4.11 shows that the swelling potential is 4.5 percent corresponding to 1 kPa. The swelling pressure is 35 kPa corresponding to the zero-swelling strain. The test results show that the clayey soil shows a medium degree of expansion as per Table 2.3, reported by (Seed and Lundgren, 1962).
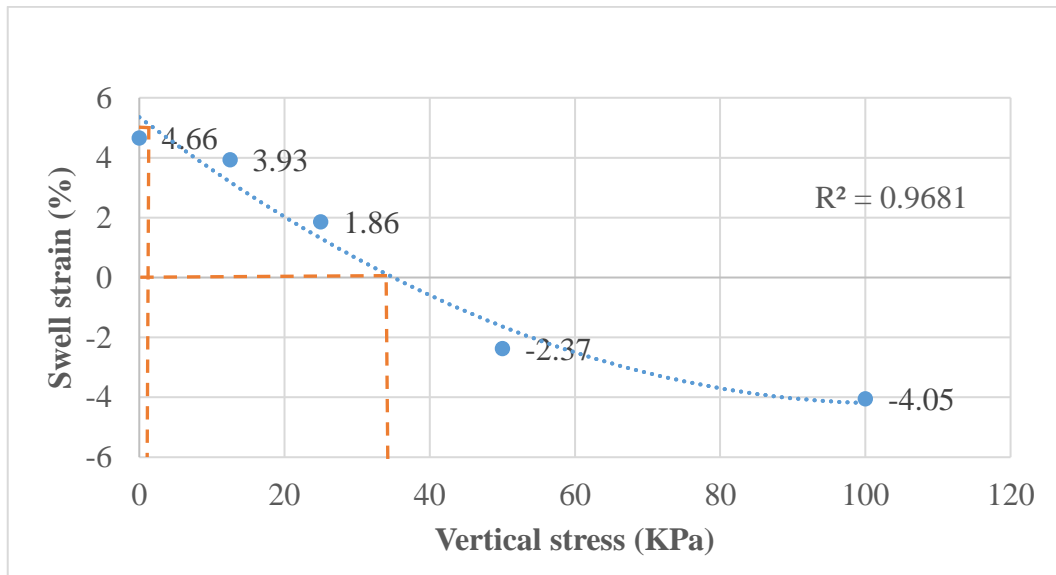


Figure 4.11**:** Vertical stress vs strain of odometer for swelling test

### 4.2.9. Activity

The activity of the silty clay sample is estimated to be 0.76. The clay sample falls in a category of normal active soil (Table 2.4). According to the activity value and the plasticity index (P.I) and clay fraction relationships (Figure 2.1), the soil is classified as illite. Illite has the swelling potential more than kaolinite and less than montmorillonite (Holeman, 1965).

### 4.2.10. Maximum and minimum void ratio

The maximum and minimum void ratios ($e_{max}$ and $e_{min}$) of sandy soil are determined to be 0.80 and 0.53 respectively, with maximum and minimum dry unit weights ($\gamma_{dmax}$ and $\gamma_{dmin}$) of 17.06 kN/m$^3$ and 14.5 kN/m$^3$ respectively. As per Equation 3.5, the dry unit weight is observed to be15.8 kN/m$^3$ at the natural state for the relative density of 55 percent.

## 4.3. Polythene sheet characterization

### 4.3.1. Tensile strength

The tensile strength of the polythene sheet is 6.5 MPa at the tensile elongation of 7 percent, obtained from the laboratory test. The tensile modulus of elasticity (E) is calculated from Figure 4.12, estimated to be107 MPa.
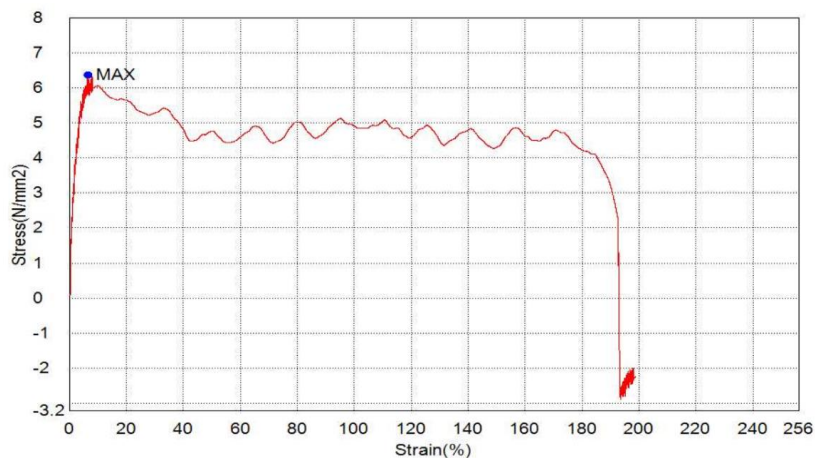


Figure 4.12**:** Stress versus strain graph of polythene sheet

## 4.4. Small scale physical model tests and verification of FEM

(Abu-Farsakh et al., 2008) tested the suitability of the finite element model (Plaxis 2D) with the small-scale laboratory model test results for a square footing to conduct a detailed analysis of the reinforced soil foundation. This study applies similar approach validating the numerical simulation test data with small scale physical model results to examine the behavior of polythene reinforced soft soil foundation as shown in Figures 4.13 - 4.15.

### 4.4.1. Only soft clay test

The bearing pressure, footing settlement, and relative settlement relationships of the soft clay for both laboratory and numerical simulation test results are shown in Figure 4.13. The relative settlement is defined as the ratio between the settlement and the width of the footing. During this test, no particular failure pattern is observed therefore, the ultimate bearing capacity is determined corresponding to 10 percent of the *s/B* ratio. As shown in Figure 4.13, the laboratory and simulation tests data are overlapping to each other, providing the ultimate bearing capacity of 61 kPa and 65 kPa respectively, which means that the results obtained from both approaches are in good agreement to each other.
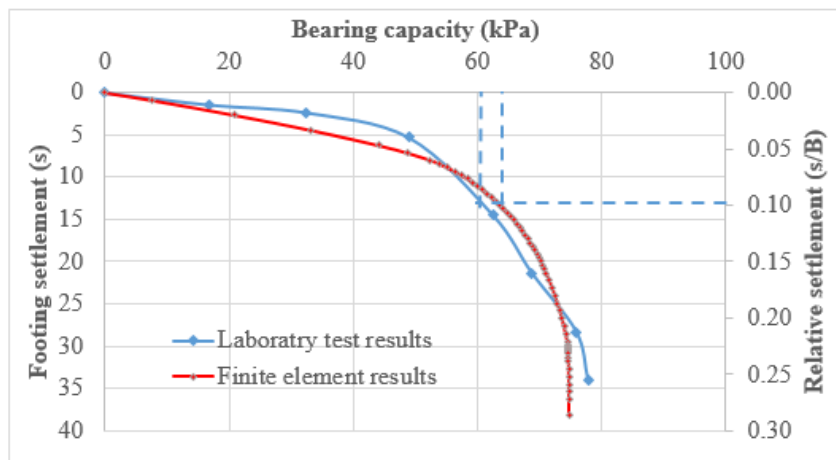


Figure 4.13: Bearing pressure-footing settlement curve for the soft clay by the laboratory and finite element tests

**4.4.2 Granular fill over the soft clay**

The purpose of this test is to figure out the improvement in the BC due to granular fills in combination with the soft clay. The bearing capacity-settlement curves of both the numerical simulation and laboratory model tests are shown in Figure 4.14. The  FEM and small-scale laboratory analysis provides bearing capacity of 102 kPa and 93 kPa  respectively for sand overlyiny soft soil foundation, and again, a good agreement is found  between the two approaches. The percentage of improvement due to the sand  fill on the soft clay is 57 percent, giving a bearing capacity ratio of 1.6. According to (Binquet and Lee, 1975) "bearing  capacity ratio" is defined as the ratio of the BC of granular or/and geosynthetic to the BC of unreinforced soft soil foundation.
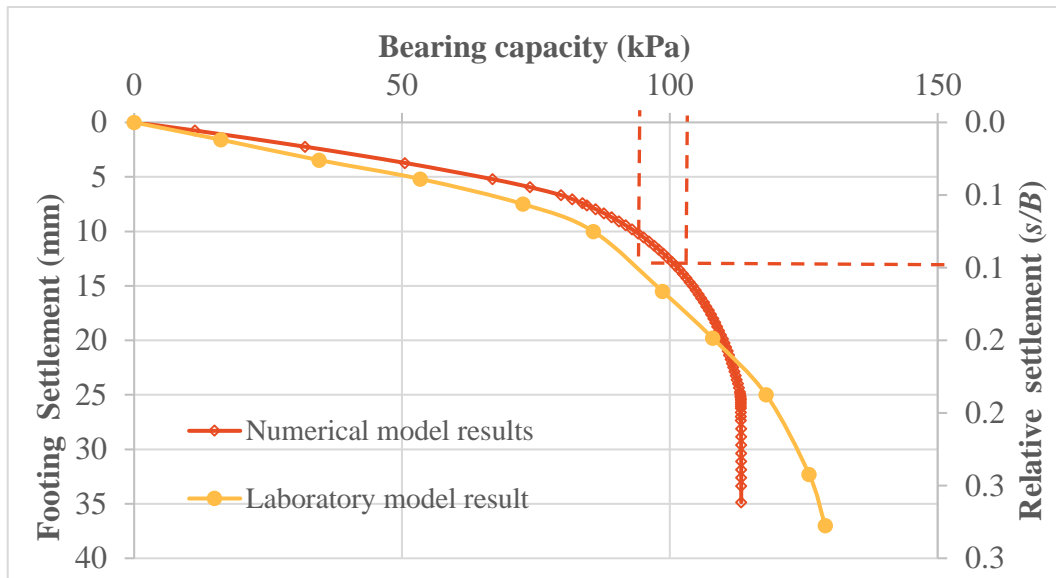


Figure 4.14**:** Bearing pressure-footing settlement curve for the sand overlying soft clay (*Ds/B*=0.75) by the laboratory and finite element tests

**4.4.3. Effect of number of polythene sheet layers**

Tests were performed in the laboratory to check  the effects of the number of the polythene sheet layers in the sand overlying soft clay foundations. With reference to the previous studies, the polythene sheets are kept; with the top layer spacing = 0.25*B*; with spacing between the consecutive layers = 0.50*B;* and  with a length of 5*B* in all these

tests. The bearing capacity increases with an increase in polythene sheeting, initially for up to three number of layers, but afterthen, a decreasing trend in bearing capacity is noted for higher number of layers (Figure 4.15). The test data was found similar to the previous researches as reported by (Binquet and Lee, 1975; Akinmusuru and Akinbolade, 1981; Guido et al., 1986). The test results shows that bearing capacity of the polythene reinforced foundation is estimated, maximum for three layers for an effective depth of 1.25$B$.
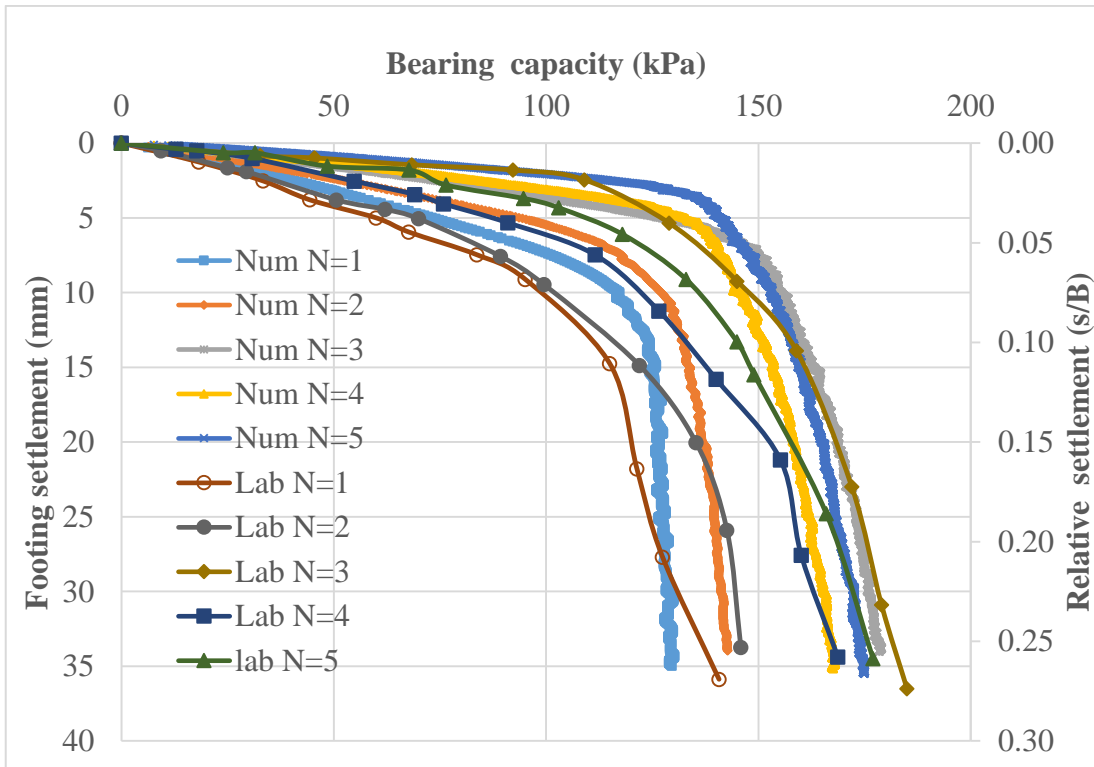


Figure 4.15: Bearing pressure-footing settlement curve for the different number of polythene sheet layers with $Ds/B$=0.75, $u/B$=0.25, and $h/B$=0.50 condition by the numerical and the laboratory model

Consequently, the UBC increases from 61 kPa (Figure 4.13) to 159 kPa (Figure 4.15) for the laboratory tests and 65 kPa (Figure 4.13) to 162 (Figure 4.15) for the numerical tests. The percentage of maximum improvement in the BC due to the

replacement of sand and the polythene sheeting is estimated to be 160 percent and 149 percent in the laboratory and numerical model tests, respectively.

## 4.5. The output of numerical model testing

### 4.5.1. Effect of thickness of the replaced material

The *BCR* curves for five different thicknesses such as $D_s/B = 0.33, 0.50, 0.67, 0.75$ and 1 are shown in Figure 4.16. It is found that the BC increases and correspondingly the settlement of the soil system reduces as sand thickness in the model increases, and this improvement is observed maximum at 0.75*B*, but after then, the insignificant improvement in BC is observed, despite of an increase in the thickness of replaced materials. Consequently, the sand layer of 0.75*B* provides the most favorable results as compared to other alternatives. The results obtained are in good agreement with (Hasanzadeh and Choobbasti, 2016).

The granular material is stronger and stiffer than the soft clay which distributes the stress to the larger area and transforms the low stress intensity to the underlying soft soil as reported by (Hasanzadeh and Choobbasti, 2016). In the current study, as the thickness of the replaced sand reaches to 0.75*B*, the entire shear failure surface develops within the replaced layer, so the maximum BC is achieved. So, in the next analysis, the thickness of upper sand layer is kept constant (0.75B) in the model to examine the other parameters, influencing the BC of composite foundations.
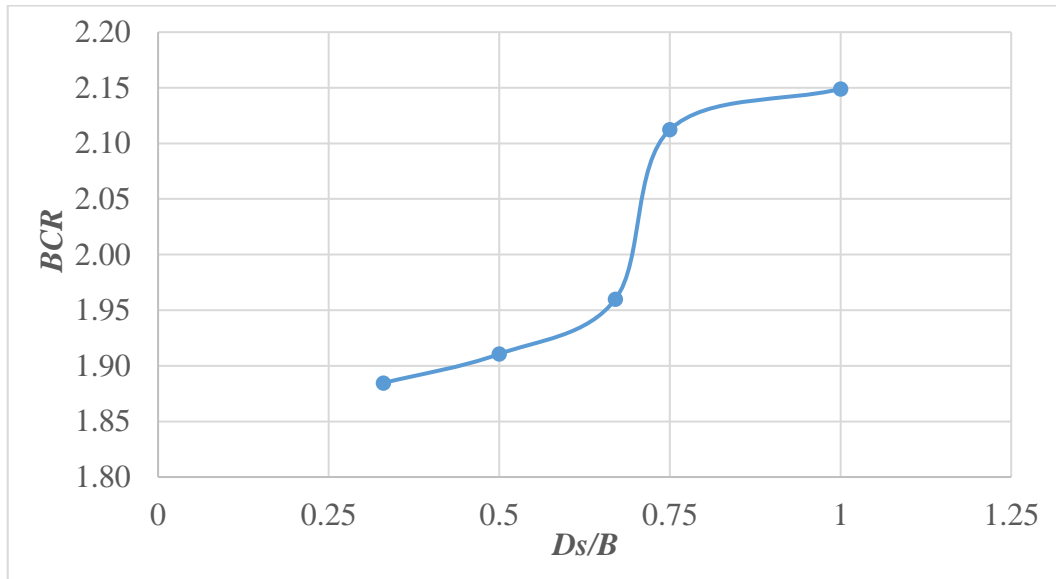
Figure 4.16: Bearing capacity ratio (*BCR*) curve between depths of replacement of the sand over soft clay to the footing width (*Ds/B*) of numerical tests.

### 4.5.2. Effect of top spacing of polythene sheet

The location of single top layer reinforcement (*u*) is examined, using the polythene reinforcement with a length of 5*B*. The bearing capacity ratio vs top layer spacing per unit width of only soft clay and sand replaced soft clay is presented in Figure 4.17. The *BCR* of the only soft clay and sand overlying soft clay increases from 2.06 to 2.12 and 2.23 to 2.39 respectively as *u* increases from 0.13*B* to 0.25*B*; and after that, it decreases and remains constant. The effect of top layer spacing is found more significant in the sand overlying soft clay to that of the only soft clay. As in Figure 4.17, the reinforcement at 0.25*B* (38.1 mm) gives peak *BCR*.

The current results are found in good agreement to the previous researches such as (Guido et al., 1986) suggested that geogrid and geotextile reinforced soil foundations provided the maximum bearing capacity at *u*=0.25*B*, and (Demir et al., 2008) described that maximum improvement in BC occurred at *u*=0.25*D* for circular footing in the soft soil foundations. (Gamal and El-Soud, 2016) reported the optimum top layer spacing of 0.25*B* for the geogrid reinforced soils in case of strip footings, while conducting the numerical study.
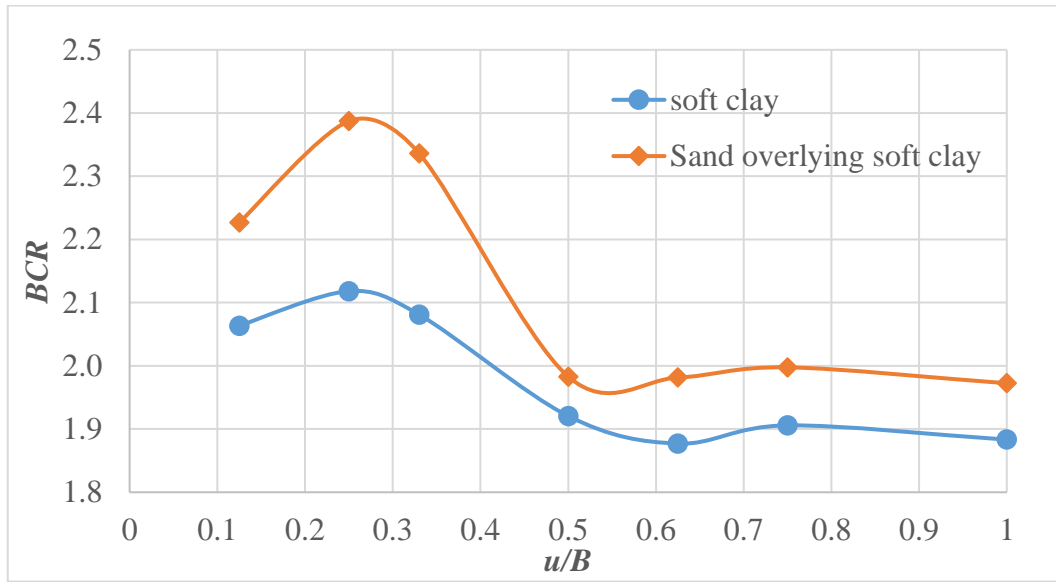
Figure 4.17: Variation of bearing capacity ratio (*BCR*) with the top layer spacing to footing width (*u/B*)

### 4.5.3. Effect of number of reinforcement layers

Numerical simulation was carried out to check the effects of the number of polythene sheet layers on the only soft clay and sand overlying soft clay foundations. A polythene sheet with a length of $5B$, with a top spacing of $0.25B$ and in-between spacing of $0.50B$ was used in these test series. The bearing capacity vs footing settlement and relative settlement curves of sand replaced soft clay and only soft clay model tests are presented in Figure 4.18 and Figure 4.19 respectively. According to the test results, the bearing capacity increases as the number of polythene reinforcement increases as expected but, after then, quite surprisingly, the bearing capacity curves bounce back, showing a decrease in the BC for higher number of polythene layers. Resultantly, the addition of polythene sheeting results in an increase in the bearing capacity up to 102 percent and 162 percent in the soft clay and sand replaced soft clay respectively.

The variations in the *BCR*s, obtained at different effective depths (*d/B*) with varying numbers of polythene layers (*N*) are shown in Figure 4.20. The *BCR* increases up to *N*=3, located at a depth of $1.25B$ and after then, it decreases and then flattens showing no increase for both sand overlying soft clay and only soft clay conditions

64

(Figure 4.20). Similar trends were reported by other researchers while conducting their researches on the composite foundations; (Binquet and Lee, 1975) for the geogrid, (Akinmusuru and Akinbolade, 1981) for the strip of fiber reinforcement and (Guido et al., 1986) for the geotextile and geogrid. (Ei Sawwaf., 2007) reported that the geogrid strengthened foundation provided the maximum improvement in BCR for three layers, while conducting the laboratory and numerical model tests.

The ultimate bearing capacity variation with the different number of polythene sheet layers (*N*) system can be explained as follow; i-) (Burd, 1995) reported that as the number of layers of polythene sheet was less, large deflection was developed in polythene layers underneath the footing. This large deflection led to the mobilization of tensile resistance and membrane action, which transferred the applied load of the footing to the polythene sheet by this mechanism. However, when the polythene layers were increased beyond three, shear failure zone was observed above the layers of reinforcement as shown in Figure 4.21. This tended to the ineffective use of tensile and membrane action of the reinforcement and resulted in a gradual reduction in bearing capacity ratio, which then remained constant, ii-) the second reason behind the reduction in the BCR was the undrained condition of the soft clay, due to which water percolated to the bottom layer of soil, which reduced the friction and membrane action of the polythene sheets.
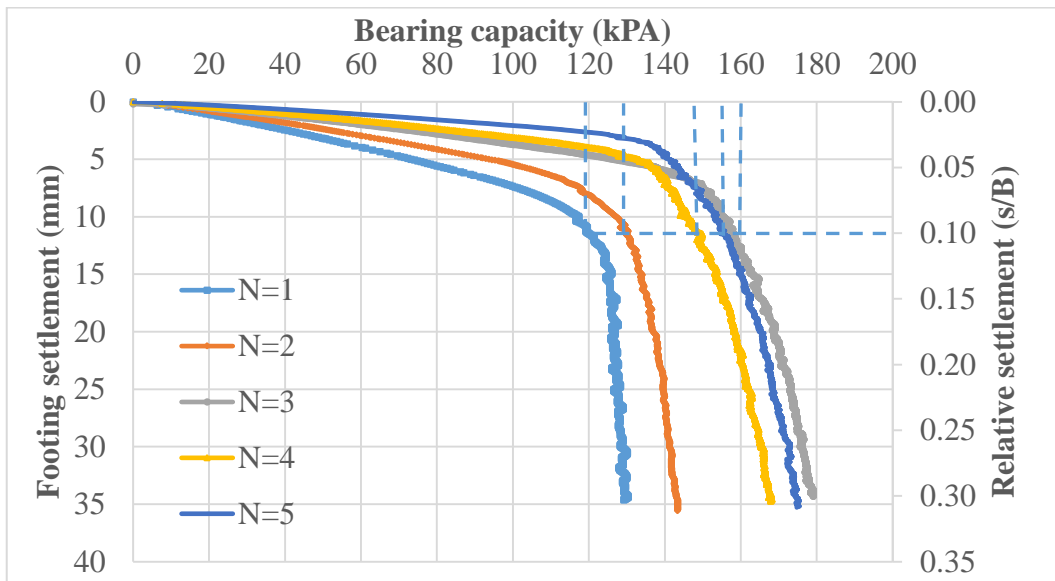
Figure 4.18: Bearing pressure-footing settlement curve for the different number of polythene sheet layers with $D_s/B$=0.75, $u/B$=0.25, and $h/B$=0.50 condition in the FEM.
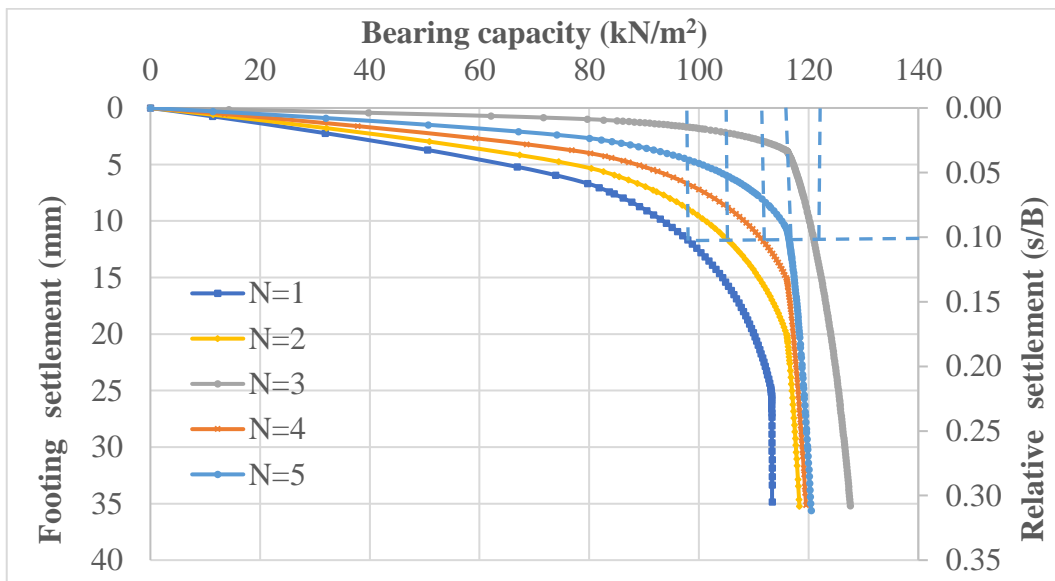


Figure 4.19: Bearing pressure-footing settlement curve for the different number of polythene sheet layers with $u/B$=0.25 and $h/B$=0.50 condition in the FEM.
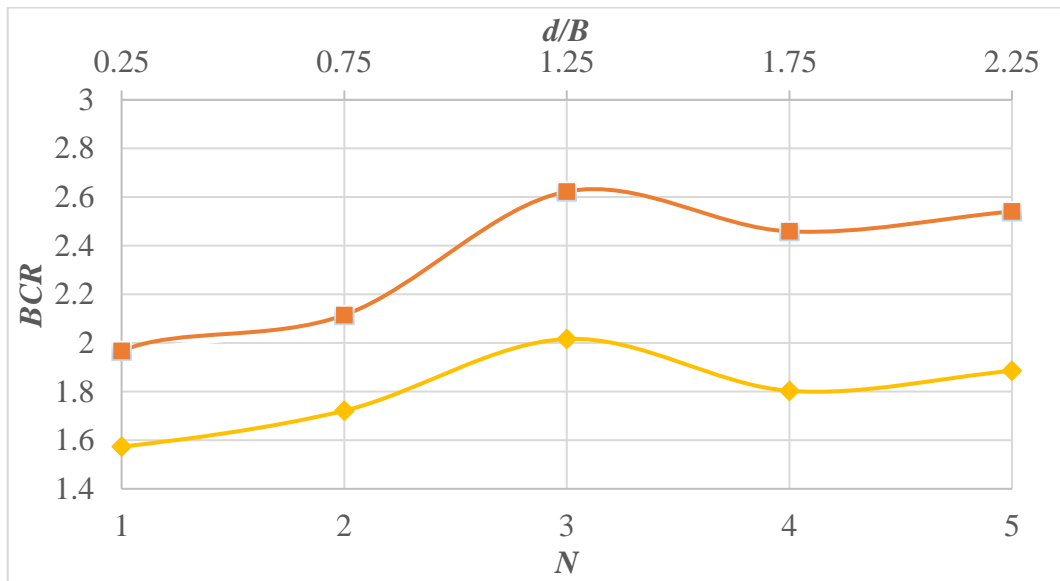
Figure 4.20: Bearing capacity ratio curve (*BCR*) between the number of layers (*N*) and depth of improvement (*d/B*) of the sand replaced soft clay and only soft clay
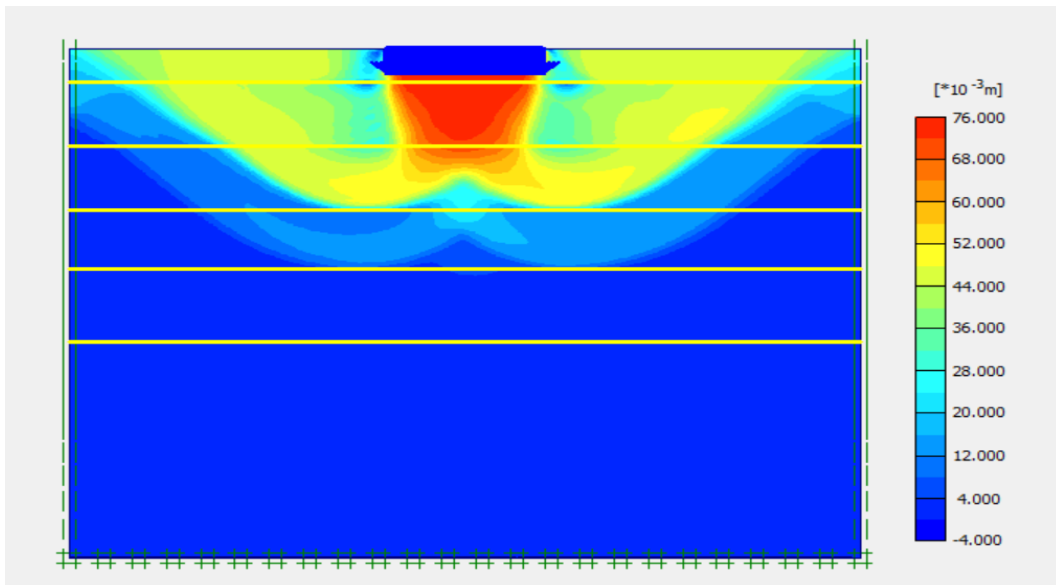


Figure 4.21: Shear failure zone of the five layers of the reinforcement in the plaxis 2-D

### 4.5.4. Effect of vertical spacing between reinforcement layers

The vertical spacing between the layers is examined using 3 polythene sheets with a length of 5*B* and a top spacing of 0.25*B* in both sand-replaced and only soft clay foundations. The variation in the *BCR*s with *h/B* is shown in Figure 4.22. The test results shows that the *BCR* increase up to 0.5*B*, but after then, it decreases in both the cases. Consequently, the best vertical spacing between the reinforcement is found to be 0.5*B*. However, in the current study, in-between spacing of the reinforcement is more significant in the sand replaced soft clay rather than the only soft clay foundations (Figure 4.22).
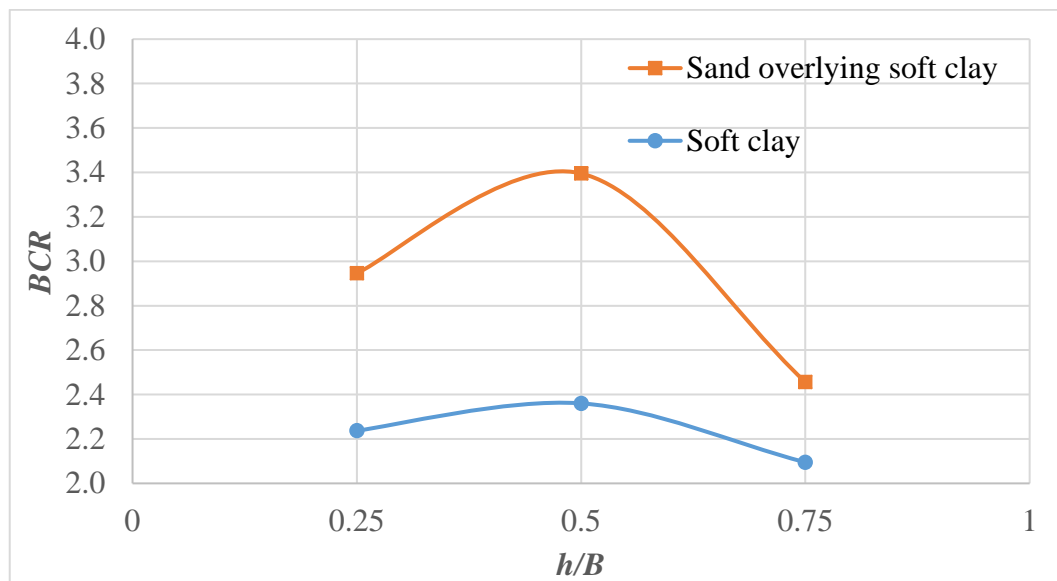


Figure 4.22: Variation of bearing capacity ratio (*BCR*) with the vertical spacing between the reinforcement layers to footing width (*h/B*)

The results are found consistent with the findings of previous researches such as; (El Sawwaf., 2007) reported that 0.5*B* was the optimum in-between spacing of the sand overlying the soft clay; (Latha and Somwanshi, 2009) proved that *h/B*=0.5 (at *N*=4) improved the maximum BC of footing in the sand; and (Bazne et al., 2015) suggested that maximum improvement occurred when the vertical spacing between the layers was 0.5*B* in geonet reinforced foundations.

### 4.5.5. Effects of length of the reinforcement

The variations in the bearing capacity ratio (*BCR*) with different lengths of polythene sheet to the footing width (*b/B*) are shown in Figure 4.23. The test results shows that as the length of the reinforcement is increased, the *BCR* increases, and this increase continues up to the reinforcement length of *5B*. The improvement is significant in the sand replaced soft clay to that of soft clay foundations. The results are similar to the finding of previous researches, in which (K. Lee et al., 1999) proved that the BCR was maximum for a length of 5-6*B* of strip footings. (Bera et al., 2005) gave the optimum width 5-7*B* for square footing, conducting regression analysis. (El Sawwaf., 2007) gave *5B*, the optimal length of the geogrid reinforced sand overlying soft clay for the square footing. (Latha and Somwanshi, 2009) determined that the optimum reinforcement width was *5B* for the square footing in sand.

In the present stsudy, the bearing capacity of polyethene reinforced foundation increased with a gradual increase in the length of the polythene sheeting due to its tensile behavior, which effectively mobilized the portion, under the shear zone of the footing as reported by (Jewell, 1996). There was an increase in the bearing capacity up to the point, the reinforcement was placed within the internal radial zone of footing, and beyond this point, the improvement was insignificant (Morel and Gourc, 1997). (Latha and Somwanshi, 2009) reported that the anchorage zone and shear zone, adjoining the sides of polythene reinforcement played their decsive roles in the determination of optimal length of the reinforcements. According to the study, the anchorage provided pull out resistance due to the additional length of reinforcement beyond the shear zone, which consequently resulted in an increase in the bearing capacity of polythene strengthened soft soil foundation.
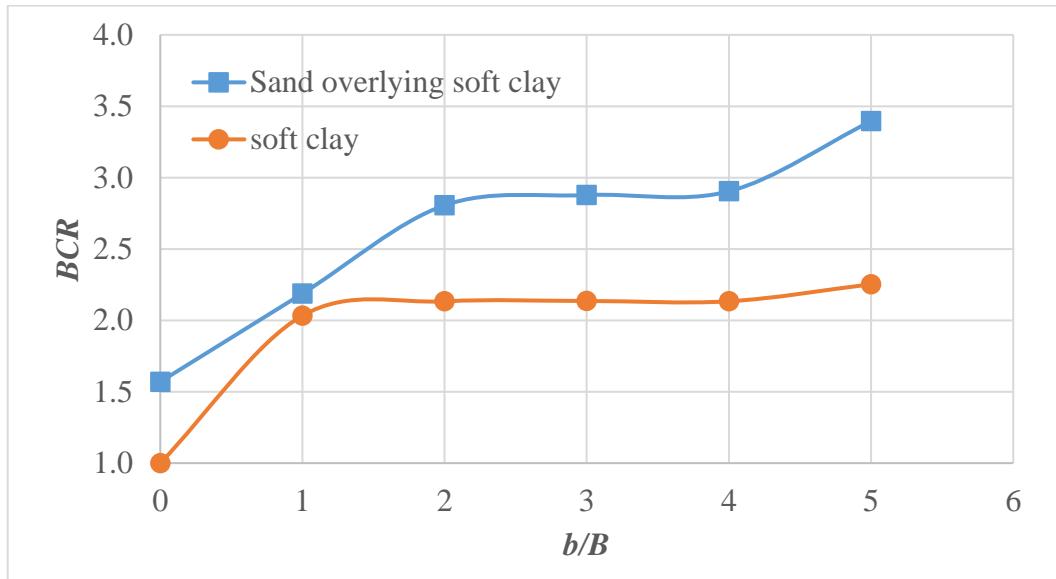
Figure 4.23: Variations of the bearing capacity ratio (*BCR*) with different lengths of polythene sheet to the footing width (*b/B*)

## 4.6. Failure mechanism of the foundation

Soft clay exhibits the punching failure in which the foundation soil is compressed under the footing without showing any bulging surface as shown in Figure 4.24. There is relatively large vertical displacement, but small horizontal displacement observed during the physical and numerical model tests. The local shear failure zone is developed in sand replaced soft clay without and with polythene sheeting. As shown in Figures 4.25 and 4.26, the stresses are distributed on a larger area in case of polythene reinforcement as compared to unreinforced soil, which consequently increases the bearing capacity (Figures  4.18 - 4.20). There is vertical compression below the surface of the footing as well as little bulging at the ground  surface. The vertical displacement is due to the punching of the junk of the sand into the soft clay, and there is dilation of the sand too, causing the horizontal displacements. During tests, no peak load, no sudden failure, and not tilting of footings were observed.
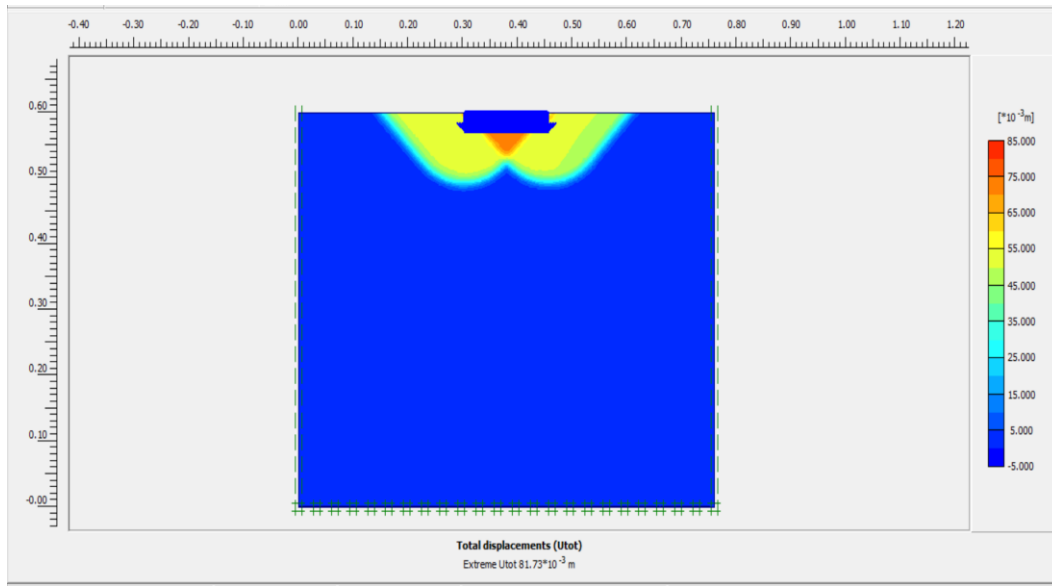
Figure 4.24**:** Shear failure zone of only soft clay
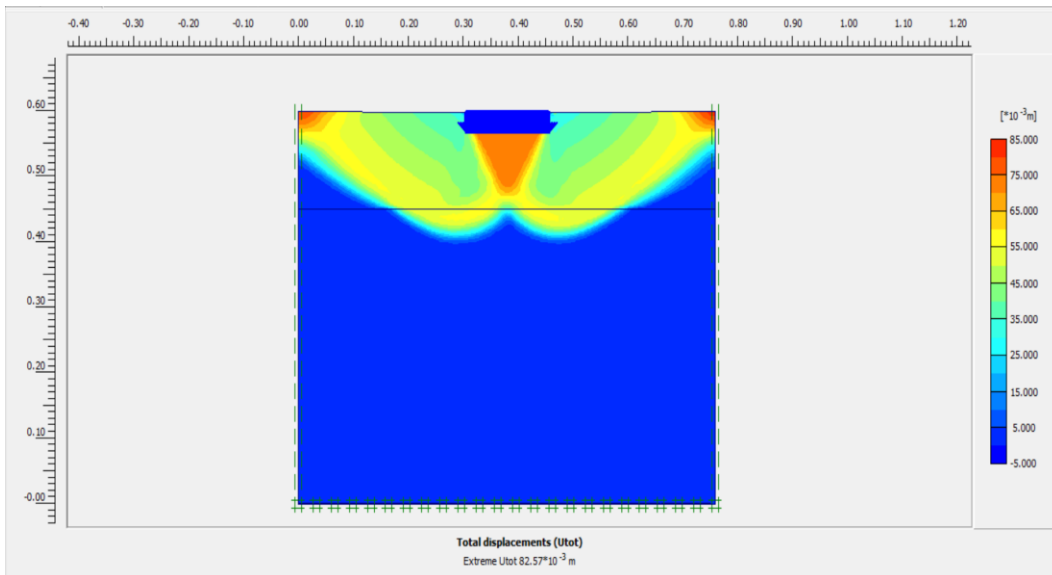


Figure 4.25**:** Shear failure zone of sand replaced soft clay (*Ds/B*=0.75)
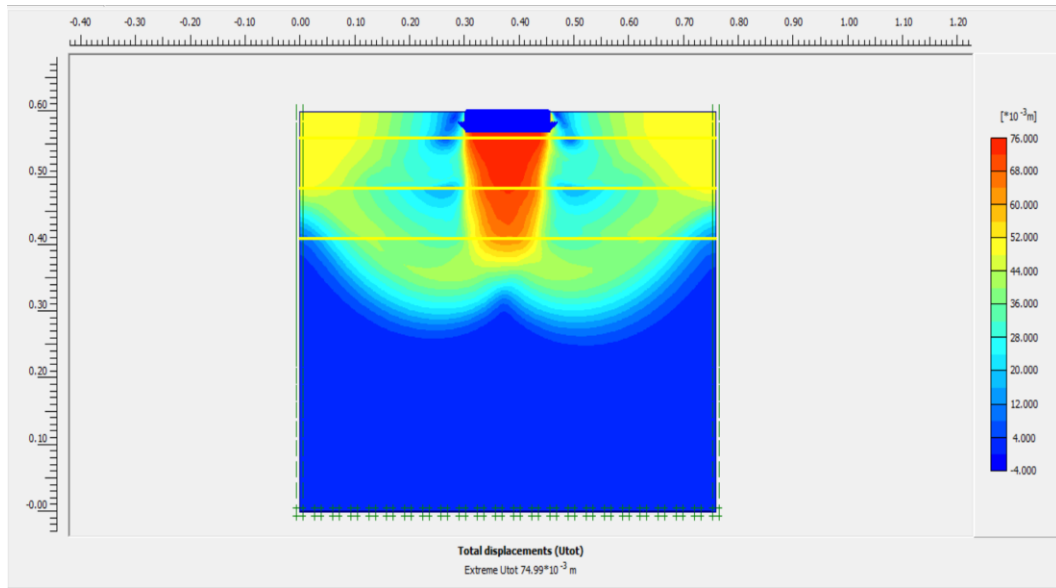
Figure 4.26: Shear failure zone sand overlying soft clay (*Ds/B*=0.33) with three layers of polythene sheet

# 5. CONCLUSIONS AND RECOMMENDATIONS

## 5.1. Conclusions

Based on the laboratory and numerical simulation test results of polythene and granular fills reinforced soft soil foundations, the following conclusions are drawn from the study:

1. It is important to consider the scale effect in the development of a small-scale physical model as it may greatly influence the reliability of the test data.

2. The soft silty clay provides a cohesion of 21.2 kPa and angle of internal friction of $5.0º$ whereas sand is a cohesionless material, giving an angle of internal friction of $42.0º$.

3. The thickness of sand layer with 0.75 times the footing width provides the most favorable results by improving 75% bearing capacity of the soft soil foundation.

4. The best top layer spacing for the single layer of reinforcement is $0.25B$ for both the sand replaced soft clay and only soft clay foundations, which increases the bearing capacity of sand replaced soft clay and soft clay up to 98% and 75% respectively to that of unreinforced foundation soil system.

5. The bearing capacity increases with an increase in the number of polythene reinforcement layers up to three, beyond this, the influence is insignificant. The percentage of maximum improvements by the polythene sheet is estimated to be 102% and 162% in the soft clay and sand replaced soft clay respectively to that of unreinforced foundation.

6. The most favorable influence depth is observed to be $1.25B$ for both polythene-reinforced in sand overlaying soft clay and only soft clay.

7. The polythene reinforcement provides the maximum benefits for in-between spacing of consecutive layers at $0.50B$ . The bearing capacity ratio ($BCR$) is found  to be 2.4 and 3.4 of the soft clay and sand replaced soft clay respectively.

8. The bearing capacity keeps on increasing with  an increase  in the length of the polythene reinforcement, which suggests examining the  reinforcement length greater than $5B$ in future studies.

## 5.2. Recommendations

Few recommendations are also drawn from the study on the basis of physical and numerical test data;

1. The  research  study  is  carried  out  without  incorporating  the  effect  of groundwater, so it is suggested to consider the effect  of groundwater on the bearing  capacity of polythene reinforced soft soil foundations.

2. There is a need to do a comparative study of polythene sheet with other geosynthetic materials such as geotextile, geomembrane, and geogrid etc., under the similar conditions.

3. It is also suggested to evaluate the performance  of polythene  reinforced soft soil foundation for different loading conditions such as inclined, eccentric, repeated or cyclic loadings.

# References

Abu-Farsakh, M., Chen, Q., Sharma, R., and Zhang, X. (2008). Large-scale model footing tests on geogrid-reinforced foundation and marginal embankment soils. *Geotechnical Testing Journal, 31*(5), 413-423.

Abu-Farsakh, M., Chen, Q., and Sharma, R. (2013). An experimental evaluation of the behavior of footings on geosynthetic-reinforced sand. *Soils and Foundations, 53*(2), 335-348.

Al-Suhaily, A. S. Improvement of Bearing Capacity of Footings on Soft Clay by Partial Soil Replacement Technique.

Al-Taie, E., Al-Ansari, N., and Knutsson, S. (2016). Evaluation of Foundation Settlement under Various Added Loads in Different Locations of Iraq Using Finite Element. *Engineering, 8*(5), 257-268.

Ashayeri, I., and Yasrebi, S. (2009). Free-swell and swelling pressure of unsaturated compacted clays; experiments and neural networks modeling. *Geotechnical and Geological Engineering, 27*(1), 137.

Asuri, S., and Keshavamurthy, P. (2016). Expansive soil characterisation: an appraisal. *INAE Letters, 1*(1), 29-33.

Barksdale, R. D., and Bachus, R. C. (1983). *Design and construction of stone columns*: Federal Highway Administration.

Belal, A., Nagy, N., and Elshesheny, A. (2015). *Numerical evaluation of bearing capacity of square footing on geosynthetic reinforced sand.* Paper presented at the Proceedings of the International Conference on Civil, Structural and Transportation Engineering.

Binquet, J., and Lee, K. L. (1975). Bearing capacity tests on reinforced earth slabs. *Journal of geotechnical and geoenvironmental engineering, 101*(ASCE# 11792 Proceeding).

Bjerrum, L. (1967). Engineering geology of Norwegian normally-consolidated marine clays as related to settlements of buildings. *Geotechnique, 17*(2), 83-118.

Bowles, L. (1996). *Foundation analysis and design*: McGraw-hill.

Brinkgreeve, R., and Shen, R. (2011). Structural Elements & Modelling Excavations in Plaxis. *Power Point Presentation File*.

Brinkgreve, R. (2002). *Plaxis: finite element code for soil and rock analyses: 2D-Version 8:[user's guide]*: Balkema.

Brown, J., and Meyerhof, G. (1969). *Experimental study of bearing capacity in layered clays.* Paper presented at the Soil Mech & Fdn Eng Conf Proc/Mexico/.

Cerato, A. B., and Lutenegger, A. J. (2007). Scale effects of shallow foundation bearing capacity on granular material. *Journal of geotechnical and geoenvironmental engineering, 133*(10), 1192-1202.

Chen, Q. (2007). An experimental study on characteristics and behavior of reinforced soil foundation.

Chung, W., and Cascante, G. (2007). Experimental and numerical study of soil-reinforcement effects on the low-strain stiffness and bearing capacity of shallow foundations. *Geotechnical and Geological Engineering, 25*(3), 265-281.

Cicek, E., Guler, E., and Yetimoglu, T. (2015). Effect of reinforcement length for different geosynthetic reinforcements on strip footing on sand soil. *Soils and Foundations, 55*(4), 661-677.

Cornforth, D. (1973). Prediction of drained strength of sands from relative density measurements *Evaluation of relative density and its role in geotechnical projects involving cohesionless soils*: ASTM International.

Das, B. M. (2013). *Advanced soil mechanics*: Crc Press.

Demir, A., Ornek, M., Laman, M., Yildiz, A., and Misir, G. (2008). *Model studies of circular foundations on soft soils.* Paper presented at the Proceedings of the 2nd International Workshop on Geotechnics of Soft Soils.

Duncan, J. M., and Buchignani, A. (1976). *An engineering manual for settlement studies*: University of California, Department of Civil Engineering.

El-kasaby, E.-s. (1991). Estimation of Guide Values for the Modulus of Elasticity of Soil. *Bulletin of the Faculty of Engineering , Assiut University, 19*, 1-7.

Fourie, A., and Potts, D. (1989). Comparison of finite element and limiting equilibrium analyses for an embedded cantilever retaining wall. *Geotechnique, 39*(2), 175-188.

Frydman, S., and Burd, H. J. (1997). Numerical studies of bearing-capacity factor N γ. *Journal of geotechnical and geoenvironmental engineering, 123*(1), 20-29.

Gamal, A., and El-Soud, S. (2016). *Numerical Modeling of Geogrid Reinforced Soil Bed under Strip Footings Using Finite Element Analysis*.

Ghalehjough, B. K., Akbulut, S., and Çelik, S. (2017). Experimental and numerical investigation on bearing capacity of granular soil affected by particle roundness.

Gouw Dr, T.-L. (2014). Common Mistakes on the Application of Plaxis 2D in Analyzing Excavation Problems. *9*, 8291-8311.

Guido, V. A., Chang, D. K., and Sweeney, M. A. (1986). Comparison of geogrid and geotextile reinforced earth slabs. *Canadian Geotechnical Journal, 23*(4), 435-440.

Hamed, J. (2001). Bearing capacity of strip foundation on a granular trench in soft clay.

Han, J. (2015). *Principles and practice of ground improvement*: John Wiley & Sons.

Hasanzadeh, A., and Choobbasti, A. (2016). Estimation Of Bearing Capacity Of Circular Footings On Clay Stabilized With Granular Soil : Case Study. *International Journal of Civil Engineering and Geo-Environmental (IJCEG), Vol.6*, pp. 47-54.

Holeman, J. N. (1965). *Clay minerals*: US Department of Agriculture, Soil Conservation Service, Engineering Division.

Huang, C.-C., and Menq, F. (1997). Deep-footing and wide-slab effects in reinforced sandy ground. *Journal of geotechnical and geoenvironmental engineering, 123*(1), 30-36.

Ibrahim, K. M. H. I. (2016). Bearing capacity of circular footing resting on granular soil overlying soft clay. *HBRC Journal, 12*(1), 71-77.

Ismail Ibrahim, K. M. H. (2016). Bearing capacity of circular footing resting on granular soil overlying soft clay. *HBRC journal, 12*(1), 71-77.

Juran, I., and Guermazi, A. (1988). Settlement response of soft soils reinforced by compacted sand columns. *Journal of Geotechnical Engineering, 114*(8), 930-943.

Kempfert, H.-G., and Gebreselassie, B. (2006). *Excavations and foundations in soft soils*: Springer Science & Business Media.

Kenny, M., and Andrawes, K. (1997). The bearing capacity of footings on a sand layer overlying soft clay. *Geotechnique, 47*(2).

Khing, K., Das, B., Puri, V., Yen, S., and Cook, E. (1994). Foundation on strong sand underlain by weak clay with geogrid at the interface. *Geotextiles and Geomembranes, 13*(3), 199-206.

Kolay, P., Kumar, S., and Tiwari, D. (2013). Improvement of bearing capacity of shallow foundation on geogrid reinforced silty clay and sand. *Journal of Construction Engineering, 2013*.

Ladd, R. (1978). Preparing test specimens using undercompaction. *Geotechnical Testing Journal, 1*(1), 16-23.

Latha, G. M., and Somwanshi, A. (2009). Bearing capacity of square footings on geosynthetic reinforced sand. *Geotextiles and Geomembranes, 27*(4), 281-294.

Lee, K., Manjunath, V., and Dewaikar, D. (1999). Numerical and model studies of strip footing supported by a reinforced granular fill-soft soil system. *Canadian Geotechnical Journal, 36*(5), 793-806.

Lee, K. L., and Singh, A. (1971). Relative density and relative compaction. *Journal of the Soil Mechanics and Foundations Division, 97*(7), 1049-1052.

Lutenegger, A. J., and Adams, M. T. (1998). Bearing capacity of footings on compacted sand.

Madhav, M., and Vitkar, P. (1978). Strip footing on weak clay stabilized with a granular trench or pile. *Canadian Geotechnical Journal, 15*(4), 605-609.

Mandal, J., and Sah, H. (1992). Bearing capacity tests on geogrid-reinforced clay. *Geotextiles and Geomembranes, 11*(3), 327-333.

Merifield, R., Sloan, S., and Yu, H. (1999). Rigorous plasticity solutions for the bearing capacity of two-layered clays. *Geotechnique, 49*(4), 471-490.

Meyerhof, G. (1974). Ultimate bearing capacity of footings on sand layer overlying clay. *Canadian Geotechnical Journal, 11*(2), 223-229.

Meyerhof, G., and Hanna, A. (1978). Ultimate bearing capacity of foundations on layered soils under inclined load. *Canadian Geotechnical Journal, 15*(4), 565-572.

Mohan, D., and Goel, R. (1959). Swelling pressures and volume expansion in Indian black cotton soils. *Journal of Institution of Engineers (India)*, 58-62.

Mosallanezhad, M., and Moayedi, H. (2017). Comparison analysis of bearing capacity approaches for the strip footing on layered soils. *Arabian Journal for Science and Engineering, 42*(9), 3711-3722.

Ornek, M., Demir, A., Laman, M., and Yildiz, A. (2012). Numerical analysis of circular footings on natural clay stabilized with a granular fill. *Acta geotechnica slovenica, 1*, 61-75.

Osman, A., and Bolton, M. (2005). Simple plasticity-based prediction of the undrained settlement of shallow circular foundations on clay. *Géotechnique., 55*(6), 435-447.

Ouria, A., and Mahmoudi, A. (2018). Laboratory and numerical modeling of strip footing on geotextile-reinforced sand with cement-treated interface. *Geotextiles and Geomembranes, 46*(1), 29-39.

Sakti, J. P., and Das, B. M. (1987). Model tests for strip foundation on clay reinforced with geotextile layers. *Transportation Research Record*(1153).

Seed, H. B., and Lundgren, R. (1962). Prediction of swelling potential for compacted clays. *Journal of the Soil Mechanics and Foundations Division, 88*(3), 53-88.

Seed, H. B., Woodward, R. J., and Lundgren, R. (1966). Fundamental aspects of the Atterberg limits. *Journal of Soil Mechanics & Foundations Div, 92*(Closure).

Sharma, R., Chen, Q., Abu-Farsakh, M., and Yoon, S. (2009). Analytical modeling of geogrid reinforced soil foundation. *Geotextiles and Geomembranes, 27*(1), 63.

Sherif, M. A., and Burrous, C. M. (1969). Temperature effects on the unconfined shear strength of saturated, cohesive soil. *Effects of Temperature and Heat on Engineering Behavior of Soils, Special report, 103*, 267-272.

Shin, E. C., Das, B. M., Puri, V., Yen, S.-C., and Cook, E. E. (1993). Bearing capacity of strip foundation on geogrid-reinforced clay. *Geotechnical Testing Journal, 16*(4), 534-541.

Skempton, A. (1953). The colloidal activity of clays. *Selected papers on soil mechanics*, 106-118.

Smith, C., Hadas, A., Dan, J., and Koyumdjisky, H. (1985). Shrinkage and Atterberg limits in relation to other properties of principal soil types in Israel. *Geoderma, 35*(1), 47-65.

Tafreshi, S. M., and Dawson, A. (2010). Comparison of bearing capacity of a strip footing on sand with geocell and with planar forms of geotextile reinforcement. *Geotextiles and Geomembranes, 28*(1), 72-84.

Tavangar, Y., and Shooshpasha, I. (2016). Experimental and numerical study of bearing capacity and effect of specimen size on uniform sand with medium density, reinforced with nonwoven geotextile. *Arabian Journal for Science and Engineering, 41*(10), 4127-4137.

Trautmann, C. H., Kulhawy, F. H., and Longo, V. J. (1987). *CUFAD: A Computer Program for Compression and Uplift Foundaton Analysis and Design.* Paper presented at the Foundation Engineering: Current Principles and Practices.

Tyler, S. W., and Wheatcraft, S. W. (1992). Fractal scaling of soil particle-size distributions: analysis and limitations. *Soil Science Society of America Journal, 56*(2), 362-369.

Vesic, A. S. (1975). Bearing capacity of shallow foundations. *Foundation engineering handbook*.

Vilas, M., and Moniuddin, M. K. (2015). Finite Element Analysis of Soil Bearing Capacity using Plaxis. *International Journal of Engineering Research & Technology, 4*(6).

Viswanadham, B., Phanikumar, B., and Mukherjee, R. (2009). Effect of polypropylene tape fibre reinforcement on swelling behaviour of an expansive soil. *Geosynthetics International, 16*(5), 393-401.

Wayne, M. H., Han, J., and Akins, K. (1998). *The design of geosynthetic reinforced foundations.* Paper presented at the Geosynthetics in foundation reinforcement and erosion control systems.

Young, A. G., McClelland, B., and Quiros, G. W. (1988). In-situ vane shear testing at sea *Vane Shear Strength Testing in Soils: Field and Laboratory Studies*: ASTM International.

Zhou, H., and Wen, X. (2008). Model studies on geogrid-or geocell-reinforced sand cushion on soft soil. *Geotextiles and Geomembranes, 26*(3), 231-238.

Zukri, A., Nazir, R., and Mender, F. N. (2017). *An experimental study on stabilization of Pekan clay using polyethylene and polypropylene.* Paper presented at the AIP Conference Proceedings.

El Sawwaf, M. A. (2007). Behavior of strip footing on geogrid-reinforced sand over a soft clay slope. *Geotextiles and Geomembranes*, *25*(1), 50-60.